Impact of protein binding on receptor occupancy: A two-compartment model

Lambertus A. Peletier, Neil Benson, Piet H. van Der Graaf

Impact of protein binding on receptor occupancy: A two-compartment model

Lambertus A. Peletier, Neil Benson, Piet H. van der Graaf

PII: S0022-5193(10)00278-X
DOI: doi:10.1016/j.jtbi.2010.05.035
Reference: YJTBI6014

To appear in: *Journal of Theoretical Biology*

Received date: 23 March 2010
Revised date: 26 May 2010
Accepted date: 27 May 2010

Cite this article as: Lambertus A. Peletier, Neil Benson and Piet H. van der Graaf, Impact of protein binding on receptor occupancy: A two-compartment model, *Journal of Theoretical Biology*, doi:10.1016/j.jtbi.2010.05.035

Impact of Protein Binding on Receptor Occupancy: a Two-Compartment Model

Lambertus A. Peletier [1] , **Neil Benson** [2] **and Piet H. van der Graaf** [3]

Abstract

In this paper we analyse the impact of protein- and lipid- and receptor-binding on receptor occupancy in a two-compartment system, with proteins in both compartments and lipids and receptors in the peripheral compartment only. We do this for two manners of drug administration: a bolus administration and a constant rate infusion, both into the central compartment. We derive explicit approximations for the time-curves of the different compounds valid for a wide range of realistic values of rate constants and initial concentrations of proteins, lipids, receptors and the drug. These approximations are used to obtain both qualitative and quantitative insight into such critical properties as the distribution of the drug over the two compartments, the maximum receptor occupancy and the area under the drug-receptor complex curve. In particular we focus on assessing the impact of the dissociation constants, K_P, K_L and K_R of the drug with, respectively, the proteins, the lipids and the receptors, the permeability and the surface area of the membrane between compartments, and the rate the drug is eliminated from the system.

1 Introduction

Drugs are typically designed to bind to a given molecular target or subset of targets. However, the same drugs often also bind to lipids and proteins and need to cross biological membranes to access the target. Developing a better quantitative understanding of the impact of these phenomena on drug interaction with a target is highly desirable (cf. Berezhkovskiy (2010) and Schmidt (2010)).

Against this background, we investigate the impact of proteins and lipids on the effectiveness of drugs, measured by the area under the curve of the receptor occupancy ($AUCRO$) by the drug. In an earlier study by Peletier, Benson and Van der Graaf (2009), hereafter referred to as PBG, this issue was taken up in the context of a simple situation: a one-compartment system and a single protein. We demonstrated that a certain amount of protein binding could be beneficial rather than deleterious to receptor binding when measured over time, such as by the $AUCRO$ over a 12 or 24 hour period. Specifically, for realistic rate constants and concentrations, we obtained sharp estimates for the optimal value of the protein binding $K_P = k_{\mathrm{Pb}}/k_{\mathrm{Pf}}$ in terms of the $AUCRO$, where k_{Pf} and k_{Pb} are the forward and the backward rate constants of the protein binding.

[1]Mathematical Institute, Leiden University, PO Box 9512, 2300 RA Leiden, The Netherlands, Tel: +31-71-5146864; Fax: +31-71-5140979; peletier@math.leidenuniv.nl - Corresponding author

[2]Pfizer Global Research & Development, Department of Pharmacokinetics, Dynamics and Metabolism, IPC 654, Sandwich CT13 9NJ, United Kingdom; Neil.Benson@pfizer.com

[3]Pfizer Global Research & Development, Department of Pharmacokinetics, Dynamics and Metabolism, IPC 654, Sandwich CT13 9NJ, United Kingdom; Piet.Van.Der.Graaf@pfizer.com

In the present paper we extend this analysis to a more complex and realistic situation. (*i*) We consider a system distributed over two compartments, a central compartment, here referred to as the *plasma compartment*, and a peripheral compartment, called the *brain compartment*, and (*ii*) we assume that the plasma compartment contains proteins and that the brain compartment contains the same proteins, but also receptors and lipids. We assume that the binding to the proteins and the receptors is reversible and that in both compartments the rate constants of the drug with respect to the proteins are the same. The binding kinetics of the drugs to target receptors and proteins can be measured using a range of well developed techniques such as surface plasmon resonance (Rich et al., (2001)) and competition assays (Motulsky et al., (1984)) as discussed in PBG. Methods for accounting for the binding of drugs to lipids in the body have been reported in the literature (cf. Poulin et al, (2000)), assuming that drug binds to lipids according to a simple one-step reversible reaction (as shown in Figure 1).

The physico-chemical properties of a drug (for example a moderate to strong base) and the existence of different lipids such as acidic and neutral phospholipid and neutral lipid can be accounted for by using equations that estimate ionised and un-ionised concentrations (cf. Rodgers et al., (2005)). The binding of a particular drug to lipid, in non-adipose tissues, is typically estimated using the $\log P$ of the drug (i.e. the logarithm of the water:octanol partition coefficient for the non-ionised drug), with typical values for drugs lying in the range -0.4 to $+5.6$ (cf. Ghose et al., (1999)). Estimates of tissue lipid composition are available in the literature.

We consider the situation in which the drug is supplied to the plasma compartment and can enter the brain compartment through the membrane separating these compartments. We assume that *either* the drug cannot leave the brain except through the membrane, *or* there exists an additional route along which drug can flow from the brain to the plasma compartment. We are interested in the receptor occupancy in the brain compartment, and the way it is impacted by the proteins and the lipids. We shall mainly focus on the drug being administered through a bolus dose, although we shall obtain some results for when drug is administered through a constant-rate infusion.

In Figure 1 we give a schematic description of the first model, when between the compartments, drug is only exchanged through the membrane. The schematic description of the second model is the same, except that an arrow from the brain compartment into the plasma compartment is added, indicating uni-directional flow of free drug.

The resulting models lead to systems of 10 nonlinear ordinary differential equations (ode's). Thanks to the conservation of proteins, receptors and lipids in the individual compartments this system can be reduced to a system of 6 ode's. The resulting nonlinear systems are still complex. However, as in PBG, thanks to the considerable differences between different concentrations and rate constants, it is possible to distinguish distinct time scales over which sub-systems are in quasi-equilibrium and the full 6-equation system can be simplified to systems, which, as it turns out, can often be solved explicitly.

Using these models we shall explore the complex interplay of drug permeability and drug binding to receptors, lipids and proteins; in this context we shall show how binding to lipids and protein influences time to equilibrium, explore the consequences of steady state dosing and evaluate the impact of any clearance processes from the brain. In addition,

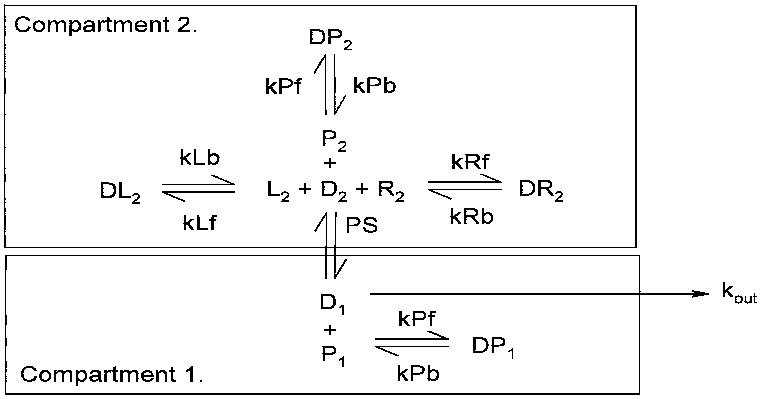

Figure 1: Schematic description of the model. Compartment 1 is the central compartment (e.g. the plasma) and compartment 2 the peripheral (e.g. the central nervous system). D_1 and P_1 are, respectively, the drug and protein concentration in the central compartment; DP_1 is the concentration of the drug-protein complex. D_2, P_2, R_2 and L_2 are the concentrations of drug, protein, receptor, and lipid in the peripheral compartment; DP_2, DR_2 and DL_2 are the concentrations of the respective complexes of drug and protein, receptor or lipid. PS is the permeability-surface area product (see Eq. (2.13)) and k_{out} is the rate constant for removal of the drug from the plasma. Typical parameter values are given in Table 1.

the importance of on- and off-rates for binding to receptor will be explored, addressing an interesting drug discovery question as to whether the values of the individual rate constants have a strong influence on receptor occupancy, rather than the affinities.

In this paper we use volumes, concentrations and rate constants which are inspired by applications to the plasma-brain system.

2 The basic model

In the model shown in Figure 1, the drug D_1 in the plasma compartment and D_2 in the brain compartment[4], binds reversibly to, respectively, the proteins P_1 in the plasma compartment and P_2 in the brain compartment. In the latter compartment it also binds reversibly to the lipids L_2 and the receptors R_2 in that compartment. Thus, the drug forms complexes with the proteins, DP_1 and DP_2, and with the lipids DL_2 and the receptors DR_2. It is assumed that proteins, lipids and receptors, and their complexes, cannot cross the membrane between the two compartments.

The drug is assumed to be introduced into the plasma compartment through an iv bolus administration, passes through the membrane that separates the two compartments and distributes itself over the two compartments. Finally, it flows out of the plasma compartment according to a first order process.

Assuming equilibrium reactions between the different species, the two-compartment

[4]The subscripts 1 and 2 refer to respectively, the plasma and the brain compartment

model shown in Figure 1 is described by the following set of reaction equations:

$$D_i + P_i \underset{k_{\mathrm{Pb}}}{\overset{k_{\mathrm{Pf}}}{\rightleftarrows}} DP_i, \qquad K_P = \frac{k_{\mathrm{Pb}}}{k_{\mathrm{Pf}}}, \qquad i = 1, 2 \tag{2.1}$$

where we assume that the on- and off-rates are the same in both compartments, and

$$D_2 + R_2 \underset{k_{\mathrm{Rb}}}{\overset{k_{\mathrm{Rf}}}{\rightleftarrows}} DR_2, \qquad K_R = \frac{k_{\mathrm{Rb}}}{k_{\mathrm{Rf}}} \tag{2.2}$$

$$D_2 + L_2 \underset{k_{\mathrm{Lb}}}{\overset{k_{\mathrm{Lf}}}{\rightleftarrows}} DL_2, \qquad K_L = \frac{k_{\mathrm{Lb}}}{k_{\mathrm{Lf}}} \tag{2.3}$$

In addition, drug is eliminated from the plasma compartment through a first order process:

$$D_1 \xrightarrow{k_{\mathrm{out}}} -k_{\mathrm{out}} D_1. \tag{2.4}$$

In Table 1 we give typical values of the rate constants:

Table 1: Rate constants and PS

k_{Pf}	k_{Pb}	k_{Rf}	k_{Rb}	k_{Lf}	k_{Lb}	k_{out}	PS
10	1000	10	10^{-2}	10	100	2×10^{-2} 1/sec	10 L/h = 1/360 L/sec

where the forward rate constants are measured in $\mu\mathrm{M}^{-1}\mathrm{sec}^{-1}$ and the backward rate constants in sec^{-1}. The values of k_{Pf} and k_{Pb} correspond to typical values for *human serum albumin* (HSA) (cf. Rich et al. (2001) and Karlsson et. al. (2000)) and we simplify by assuming one binding site per HSA molecule. For the values of k_{Lf} and k_{Lb} we refer to Gohse et al. (1999) and the values of k_{Rf} and k_{Rb} are typical for drug binding to receptor (cf. Tummino and Copeland (2008)). Finally, in conjunction with the parameter values from Tables 1 and 2, the value of k_{out} is associated with a half-life of 15 hours. Note that for the values listed in Table 1,

$$K_P = 100 \ \ \mu\mathrm{M}, \qquad K_R = 10^{-3} \ \ \mu\mathrm{M} \qquad \text{and} \qquad K_L = 10 \ \ \mu\mathrm{M}. \tag{2.5}$$

Typical values of the *permeability-surface area product* PS of the membrane range from 0.2 to 22 L/h in man (see below near equation (2.12) and the Discussion). In our simulations we have chosen a permeability in the middle of this range. In the discussion we shall briefly dwell on the impact of a low and high permeability-surface area product.

For the volumes V_1 and V_2 of, respectively, the plasma and the brain compartment we take the values pertaining to plasma and brain volume in man, i.e., $V_1 = 5$ L and $V_2 = 1.4$ L.

We denote the initial concentrations by

$$\begin{aligned} &P_i(0) = P_{i,0}, \qquad R_2(0) = R_{2,0}, \qquad L_2(0) = L_{2,0}, \qquad D_i(0) = D_{i,0}, \\ &DP_i(0) = 0, \qquad DR_2(0) = 0, \qquad DL_2(0) = 0 \qquad (i = 1, 2) \end{aligned} \tag{2.6}$$

In Table 2 we give values of the initial concentrations used in our simulations.

Table 2: Initial concentrations (in μM)

$P_{1,0}$	$P_{2,0}$	$R_{2,0}$	$L_{2,0}$	$D_{1,0}$	$D_{2,0}$
750	3	10^{-3}	1000	10	0

These data are taken from the following sources: for $P_{1,0}$ we refer to Guyton et al. (1996), for $P_{2,0}$ to Felgenhauer (1974), $R_{2,0}$ is a typical value for a low receptor concentration, and for $L_{2,0}$ we refer to Rouser et al. (1968). In our simulations we assume that there are no lipids or receptors in the plasma compartment.

The dynamics of this complex of chemical reactions and mass transfer between compartments is described by the following set of differential equations in which P_1, P_2, DP_1, DP_2, R_2, DR_2, L_2, DL_2, D_1 and D_2 now denote the concentrations of these compounds (i.e., $P_i = [P_i]$, $DP_i = [DP_i]$ etc.).

Proteins in the plasma:

$$\begin{cases} \dfrac{dP_1}{dt} = -k_{\mathrm{Pf}} D_1 \cdot P_1 + k_{\mathrm{Pb}} DP_1 \\ \dfrac{dDP_1}{dt} = +k_{\mathrm{Pf}} D_1 \cdot P_1 - k_{\mathrm{Pb}} DP_1 \end{cases} \tag{2.7}$$

and in the **brain**

$$\begin{cases} \dfrac{dP_2}{dt} = -k_{\mathrm{Pf}} D_2 \cdot P_2 + k_{\mathrm{Pb}} DP_2 \\ \dfrac{dDP_2}{dt} = +k_{\mathrm{Pf}} D_2 \cdot P_2 - k_{\mathrm{Pb}} DP_2 \end{cases} \tag{2.8}$$

Receptors in the brain

$$\begin{cases} \dfrac{dR_2}{dt} = -k_{\mathrm{Rf}} D_2 \cdot R_2 + k_{\mathrm{Rb}} DR_2 \\ \dfrac{dDR_2}{dt} = +k_{\mathrm{Rf}} D_2 \cdot R_2 - k_{\mathrm{Rb}} DR_2 \end{cases} \tag{2.9}$$

Lipids in the brain:

$$\begin{cases} \dfrac{dL_2}{dt} = -k_{\mathrm{Lf}} D_2 \cdot L_2 + k_{\mathrm{Lb}} DL_2 \\ \dfrac{dDL_2}{dt} = +k_{\mathrm{Lf}} D_2 \cdot L_2 - k_{\mathrm{Lb}} DL_2 \end{cases} \tag{2.10}$$

Drug in the plasma and the brain:

$$\begin{cases} \dfrac{dD_1}{dt} = k_+(D_2 - D_1) - k_{\mathrm{Pf}} D_1 \cdot P_1 + k_{\mathrm{Pb}} DP_1 - k_{\mathrm{out}} D_1 \\ \dfrac{dD_2}{dt} = -k_-(D_2 - D_1) - k_{\mathrm{Pf}} D_2 \cdot P_2 + k_{\mathrm{Pb}} DP_2 \\ \qquad\qquad - k_{\mathrm{Rf}} D_2 \cdot R_2 + k_{\mathrm{Rb}} DR_2 - k_{\mathrm{Lf}} D_2 \cdot L_2 + k_{\mathrm{Lb}} DL_2 \end{cases} \tag{2.11}$$

where k_+ and k_- are related to the drug transfer between the two compartments. They are given by the expressions

$$k_+ = \frac{PS}{V_1} \qquad \text{and} \qquad k_- = \frac{PS}{V_2} \tag{2.12}$$

where PS denotes the *permeability-surface area product* which is used to describe clearance between biological compartments such as the plasma and the brain. It is given by

$$PS = P \times S \tag{2.13}$$

where P denotes the permeability (cm/sec) and S the surface area of the membrane (cm^2) (see Berezhkovskiy, (2004)). Estimates for PS can be obtained experimentally in vivo in laboratory animals or in vitro systems (cf. Lundquist et al. (2002)).

Since we assume that proteins, lipids and receptors and their complexes do not cross the membrane, we have four conservation laws:

Conservation of proteins, receptors and lipids:

$$P_i + DP_i = P_{i,0} \quad (i = 1, 2), \qquad R_2 + DR_2 = R_{2,0}, \qquad L_2 + DL_2 = L_{2,0} \tag{2.14}$$

In addition if no drug is eliminated, we obtain a fifth conservation law:

Conservation of drug if $k_{\text{out}} = 0$:

$$V_1(D_1 + DP_1) + V_2(D_2 + DP_2 + DR_2 + DL_2) = V_1 D_{1,0} + V_2 D_{2,0} = A_{\text{tot}} \tag{2.15}$$

where A_{tot} is the total amount of drug in the two compartments.

The four conservation laws (2.14) make it possible to reduce the full system (2.7) - (2.11) to one of six equations (see Section 4). When there is no elimination of drug ($k_{\text{out}} = 0$) so that (2.15) holds as well, then a further reduction is possible resulting in a system of five equations.

3 Simulations

In order to acquire a first idea of the dynamics of this system with the parameter values listed in Tables 1 and 2 we present a few numerical simulations of concentration graphs of the drug and the drug-protein complex in both compartments, and the drug-lipid complex and the drug-receptor complex in the brain compartment. These simulations have been made using the software package MatLab R2009b and the stiff ordinary differential equation solvers, ode 23s and ode15s (The Math Works, Natick, MA, USA).

Since an important objective will be to understand the impact of the affinities K_P and K_L of the drug with respect to the proteins and the lipids on the receptor occupancy we begin in Figure 2 with an overall set of graphs of DR_2 *versus* time. In changing the affinities, we change the off-rates, since in practice the on-rates do not vary a great deal (see also the Discussion in Section 9).

We make the following observations:

• The drug-receptor complex DR_2 in the brain compartment shows an initial rise over a brief period of time and then decreases at a much slower rate to zero.

• The initial increase as well as the subsequent decrease of DR_2 take longer as K_P decreases and as K_L decreases.

• The maximum value of DR_2 over time drops as K_P decreases and as K_L decreases.

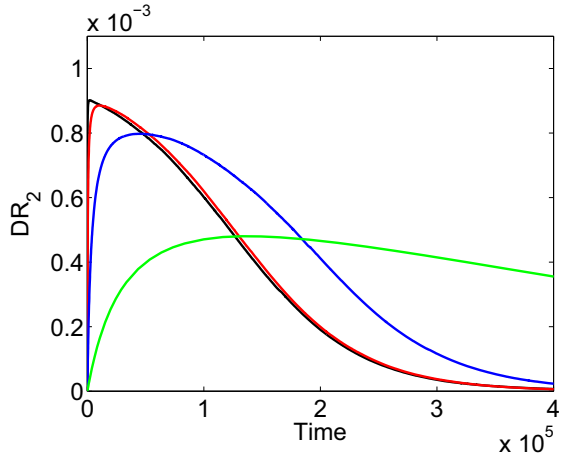

$K_P = 100,\ 10,\ 1,\ 0.1; \quad K_L = 10$

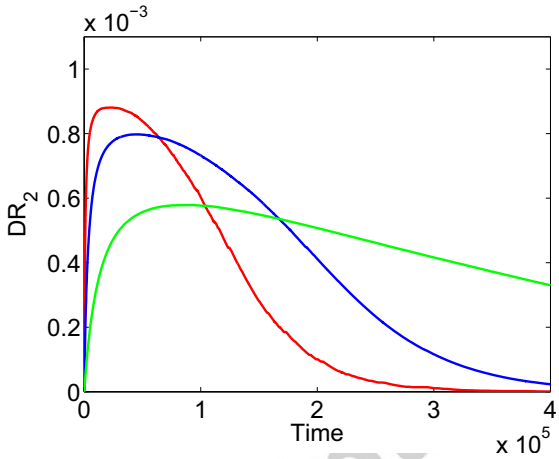

$K_L = 50,\ 10,\ 2; \quad K_P = 1$

Figure 2: Graphs of $DR_2(t)$ of the system (2.7) - (2.11) over a period of about 110 hours (12 hours = 43200 sec). On the left: k_{Pb} ranges from 1000 (black), 100 (red), 10 (blue), 1 (green), and on the right k_{Lb} ranges over 500 (red), 100 (blue), 20 (green). The other rate constants are taken from Table 1; initial concentrations are given by Table 2. Note that the blue curves in the figures on the left and the right are the same.

3.1 Concentrations in the plasma compartment

In the first two figures we investigate the behaviour of the concentration of the drug D_1 and of the drug-protein complex DP_1 in the plasma compartment after an iv bolus dose has been administered. This is done in Figures 3 and 4.

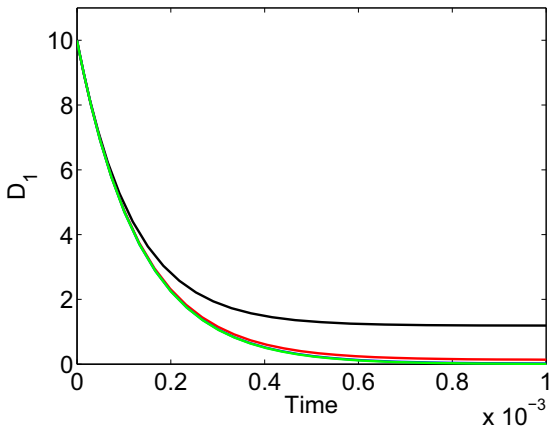

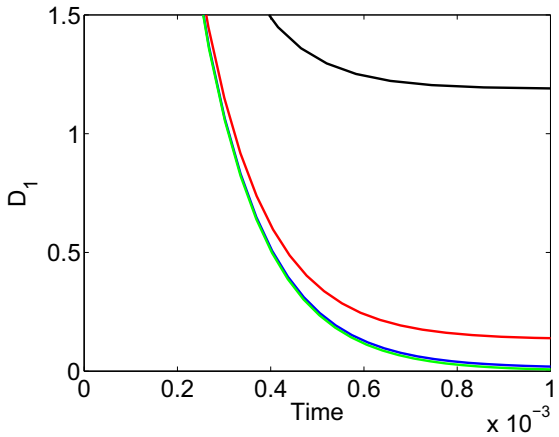

Figure 3: Graphs of drug concentration in the plasma compartment $D_1(t)$ of the system (2.7) - (2.11) over an initial period of one micro second. The rate constants and initial data given by Tables 1 and 2, for k_{Pb}=1000 (black), 100 (red), 10 (blue), 1 (green).

We see that the concentration of the drug drops very rapidly to a much lower value and that the concentration of drug-protein complex rises over a similarly short period to

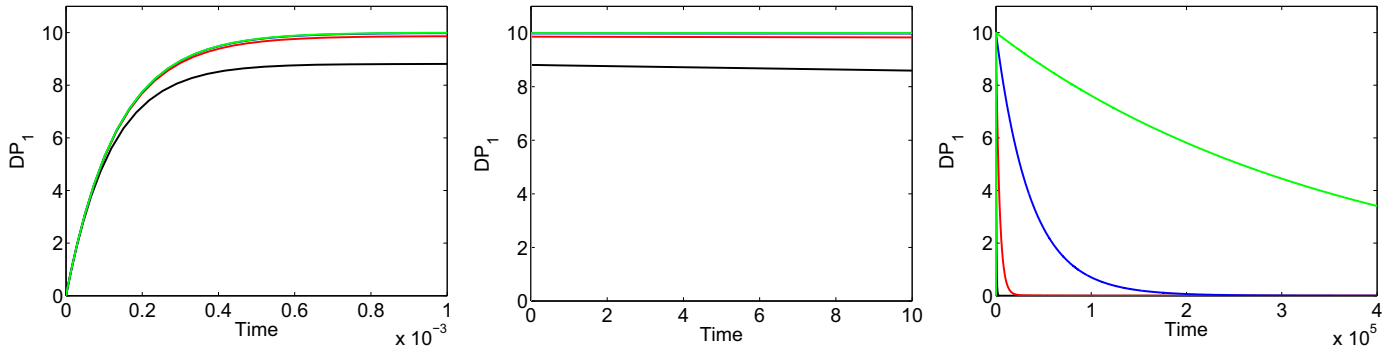

Figure 4: Graphs of the drug-protein complex concentration in the plasma compartment $DP_1(t)$ of the system (2.7) - (2.11) over three time intervals: 1 microsecond (left), 10 seconds (middle) and ± 6 days (right). The rate constants and initial data are given by Tables 1 and 2, and k_{Pb}=1000 (black), 100 (red), 10 (blue), 1 (green).

a critical value. In fact, upon close inspection, we see that over this initial period,

$$D_1(t) + DP_1(t) \approx D_{1,0}$$

i.e., drug loss through the membrane and direct elimination from the plasma compartment are negligible during this initial redistribution period. We see that as k_{Pb} decreases the free drug concentration D_1 drops to a lower level and more drug is bound to protein, i.e. DP_1 rises to a higher level.

Evidently, the half-time of the convergence to an almost constant value is about 10^{-4} sec. This agrees with the theoretical estimate of $t_{1/2} \approx \ln(2)/(k_{\mathrm{Pf}} P_{1,0})$ derived in Section 5.

After this rapid adjustment, in which - as we shall see - drug and protein reach equilibrium, drug and complex stay at approximately constant values for a relatively long period of time (cf. Figure 4). We shall often refer to this constant value as the *plateau value* of the compound. Thus, the plateau value of the free drug drops as k_{Pb} decreases and drug binds more rapidly to the proteins.

3.2 Concentrations in the brain compartment

Concentration versus time graphs of the drug-receptor complex DR_2 have been shown in Figure 2 and corresponding graphs of the drug-lipid complex DL_2 are shown in Figure 5. As in Figure 2 we vary K_P (100 - 0.1) and K_L (50 - 2) by changing k_{Pb} and k_{Lb}, whilst keeping k_{Pf} and k_{Lf} fixed (see Table 1).

Figures 2 and 5 show that as the drug binds more readily to the protein, i.e., K_P decreases, drug enters the brain compartment more slowly and we see lower, but longer lasting, complex concentrations of the drug with receptors and lipids. On the other hand, when the drug binds more readily to the lipids, i.e., K_L decreases, more drug-lipid complex is formed and the complex concentration DL_2 increases.

In Figures 2 and 5, the blue graphs on the left and on the right are taken for the same parameter values: $k_{\mathrm{Pb}} = 10$ and $k_{\mathrm{Lb}} = 100$, i.e. $K_P = 1$ and $K_L = 10$.

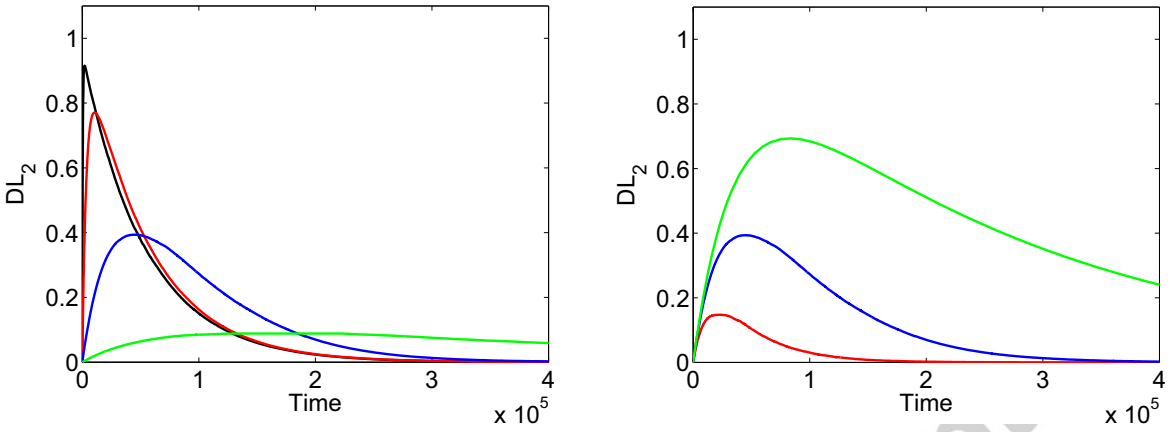

$K_P = 100,\ 10,\ 1,\ 0.1; \quad K_L = 10$ $\qquad$ $K_L = 50,\ 10,\ 2; \quad K_P = 1$

Figure 5: Graphs of $DL_2(t)$ of the system (2.7) - (2.11) over a period of around 110 hours (12 hours = 43200 sec). On the left: k_{Pb} ranges from 1000 (black), 100 (red), 10 (blue), 1 (green), and on the right k_{Lb} ranges from 500 (red), 100 (blue), 20 (green). The other rate constants are taken from Table 1; initial concentrations are given in Table 2. Note that the blue curves in the figures on the left and the right are the same. Time in seconds.

In Figure 6 we show graphs of the drug concentrations D_1 and D_2 versus time as K_P ranges from 100 to 0.1 and K_L ranges from 50 to 2. We see that the graphs of D_1 emerges from the plateau value and the drops to zero at a rate which increases as K_P increases. In Section 6 we shall show that $t_{1/2} \approx P_{1,0}/(K_P k_{\mathrm{out}})$, which agrees with the simulations in Figure 6.

Note that the graphs of D_1 and D_2 intersect at a point where $dD_2/dt \approx 0$. In light of the system (2.11) we conclude that the dominant term on the right hand side of the equation for dD_2/dt is the term involving the difference $D_1 - D_2$, i.e., in the brain compartment, the drug is approximately in equilibrium with the proteins, the receptors and the lipids.

As in Figures 2 and 5, in Figure 6 the blue curves on the left and on the right are taken for the same parameter values: $k_{\mathrm{Pb}} = 10$ and $k_{\mathrm{Lb}} = 100$, i.e. $K_P = 1$ and $K_L = 10$. Note that in the figure on the right the graphs of $D_1(t)$ approximately coincide, i.e., D_1 seems to be insensitive to changes of the affinity of the drug to the lipids. Thus, the changing affinity of the drug to the lipids primarily affects the brain compartment.

4 Reformulation of the model

Thanks to the conservation laws for proteins, receptors and lipids in both compartments, we can express the concentrations of proteins, receptors and lipids in terms of their respective complexes with the drug and thus reduce the number of independent variables in the system (2.7) - (2.11). This results in the following system of equations:

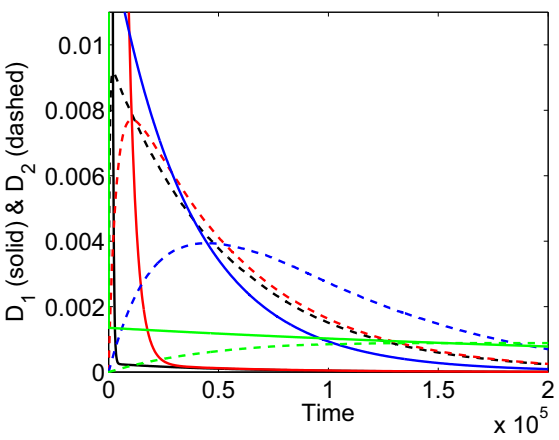

$K_P = 100,\ 10,\ 1,\ 0.1;\ K_L = 10$

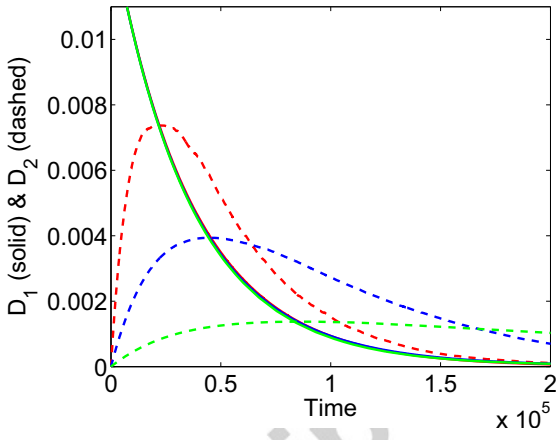

$K_L = 50,\ 10,\ 2;\ K_P = 1$

Figure 6: Graphs of $D_1(t)$ (solid) and $D_2(t)$ (dashed) of the system (2.7) - (2.11) over a period of about 55 hours (12 hours = 43200 sec) for k_{Pb}=1000 (black), 100 (red), 10 (blue), 1 (green), and on the right k_{Lb} ranges from 500 (red), 100 (blue), 20 (green). The other rate constants are given in Table 1 and initial concentrations are given in Table 2. Time in seconds.

For the plasma compartment:

$$\begin{cases} \dfrac{dDP_1}{dt} = +k_{\mathrm{Pf}} D_1 \cdot P_{1,0} - (k_{\mathrm{Pf}} D_1 + k_{\mathrm{Pb}}) DP_1 \\ \dfrac{dD_1}{dt} = k_+(D_2 - D_1) + (k_{\mathrm{Pf}} D_1 + k_{\mathrm{Pb}}) DP_1 - (k_{\mathrm{Pf}} P_{1,0} + k_{\mathrm{out}}) D_1 \end{cases} \tag{4.1}$$

For the brain compartment:

$$\begin{cases} \dfrac{dDP_2}{dt} = +k_{\mathrm{Pf}} D_2 \cdot P_{2,0} - (k_{\mathrm{Pf}} D_2 + k_{\mathrm{Pb}}) DP_2 \\ \dfrac{dDR_2}{dt} = +k_{\mathrm{Rf}} D_2 \cdot R_{2,0} - (k_{\mathrm{Rf}} D_2 + k_{\mathrm{Pb}}) DR_2 \\ \dfrac{dDL_2}{dt} = +k_{\mathrm{Lf}} D_2 \cdot L_{2,0} - (k_{\mathrm{Lf}} D_2 + k_{\mathrm{Lb}}) DL_2 \\ \dfrac{dD_2}{dt} = -k_-(D_2 - D_1) + (k_{\mathrm{Pf}} D_2 + k_{\mathrm{Pb}}) DP_2 + (k_{\mathrm{Rf}} D_2 + k_{\mathrm{Rb}}) DR_2 \\ \qquad\qquad + (k_{\mathrm{Lf}} D_2 + k_{\mathrm{Lb}}) DL_2 - (k_{\mathrm{Pf}} P_{2,0} + k_{\mathrm{Rf}} R_{2,0} + k_{\mathrm{Lf}} L_{2,0}) D_2 \end{cases} \tag{4.2}$$

Addition of the expressions for dD_1/dt and dDP_1/dt yields the balance equation for the drug in the plasma compartment:

$$\frac{d}{dt}(D_1 + DP_1) = k_+(D_2 - D_1) - k_{\mathrm{out}} D_1, \tag{4.3}$$

which states that drug leaves the plasma compartment only through direct elimination or through the membrane and it enters it only through the membrane. Similarly, for the

brain compartment we obtain

$$\frac{d}{dt}(D_2 + DP_2 + DR_2 + DL_2) = -k_-(D_2 - D_1) \tag{4.4}$$

i.e., drug only leaves or enters this compartment through the membrane.

4.1 Dimensionless variables

In order to identify the combinations of parameters which determine the dynamics of the system, we introduce dimensionless variables. For the different concentrations we take as reference values the initial concentrations of the proteins in both compartments, of the drug in the plasma compartment and of the receptors and the lipids in the brain compartment. Thus, we define the dimensionless variables

$$x_i = \frac{DP_i}{P_{i,0}}, \qquad y_2 = \frac{DR_2}{R_{2,0}}, \qquad z_2 = \frac{DL_2}{L_{2,0}}, \qquad u_i = \frac{D_i}{D_{1,0}}, \qquad i = 1, 2 \tag{4.5}$$

For the **plasma compartment** we then obtain from the system (4.1)

$$\begin{cases} \dfrac{dx_1}{dt} = +k_{\mathrm{Pf}} D_{1,0} u_1 - (k_{\mathrm{Pf}} D_{1,0} u_1 + k_{\mathrm{Pb}}) x_1, \\ \dfrac{du_1}{dt} = k_+(u_2 - u_1) - (k_{\mathrm{Pf}} P_{1,0} + k_{\mathrm{out}}) u_1 + (k_{\mathrm{Pf}} D_{1,0} u_1 + k_{\mathrm{Pb}}) \dfrac{P_0}{D_{1,0}} x_1 \end{cases} \tag{4.6}$$

and for the **brain compartment** the system (4.2) yields

$$\begin{cases} \dfrac{dx_2}{dt} = +k_{\mathrm{Pf}} D_{1,0} u_2 - (k_{\mathrm{Pf}} D_{2,0} u_2 + k_{\mathrm{Pb}}) x_2 \\ \dfrac{dy_2}{dt} = +k_{\mathrm{Rf}} D_{1,0} u_2 - (k_{\mathrm{Rf}} D_{2,0} u_2 + k_{\mathrm{Rb}}) y_2 \\ \dfrac{dz_2}{dt} = +k_{\mathrm{Lf}} D_{1,0} u_2 - (k_{\mathrm{Lf}} D_{2,0} u_2 + k_{\mathrm{Lb}}) z_2 \\ \dfrac{du_2}{dt} = k_-(u_1 - u_2) + (k_{\mathrm{Pf}} D_{1,0} u_2 + k_{\mathrm{Pb}}) \dfrac{P_{2,0}}{D_{1,0}} x_2 + (k_{\mathrm{Rf}} D_{1,0} u_2 + k_{\mathrm{Rb}}) \dfrac{R_{2,0}}{D_{1,0}} y_2 \\ \qquad + (k_{\mathrm{Lf}} D_{1,0} u_2 + k_{\mathrm{Lb}}) \dfrac{L_{2,0}}{D_{1,0}} z_2 - (k_{\mathrm{Pf}} P_{2,0} + k_{\mathrm{Rf}} R_{2,0} + k_{\mathrm{Lf}} L_{2,0}) u_2 \end{cases} \tag{4.7}$$

As in PBG we distinguish different time scales: a short time scale associated with the binding of the drug to the protein in the plasma compartment, and a longer time scale, initially associated with the dissociation of the drug receptor complex but later modified to include the effect of the permeability of the membrane. Thus, we introduce the following time variables:

$$\tau_1 = k_{\mathrm{Pb}} t \text{ (short)} \qquad \text{and} \qquad \tau_2 = k_{\mathrm{Rb}} t \text{ (long)} \tag{4.8}$$

In the following sections we assume that k_{Pb} ranges from 1000 to 1 and that k_{Lb} ranges from 500 to 20. The other constants are all taken from Table 1. Thus, K_P ranges from 100 to 0.1 and K_L from 50 to 2. The initial concentrations are taken from Table 2.

5 Dynamics in the plasma compartment

In order to study the short time dynamics in the plasma compartment, we replace the time t by the scaled time τ_1 to obtain the system

$$\begin{cases} \dfrac{dx_1}{d\tau_1} = au_1 - (au_1 + 1)x_1, \\ \dfrac{du_1}{d\tau_1} = \dfrac{k_+}{k_{\mathrm{Pb}}}(u_2 - u_1) - \left(a\dfrac{P_{1,0}}{D_{1,0}} + \dfrac{k_{\mathrm{out}}}{k_{\mathrm{Pb}}}\right)u_1 + (au_1 + 1)\dfrac{P_{1,0}}{D_{1,0}}x_1, \end{cases} \tag{5.1}$$

where

$$a = \frac{k_{\mathrm{Pf}}}{k_{\mathrm{Pb}}}D_{1,0} = \frac{D_{1,0}}{K_P} \tag{5.2}$$

Assumption 1: $k_+ = PS/V_1 \ll k_{\mathrm{Pf}}P_{1,0}$ and $k_{\mathrm{out}} \ll k_{\mathrm{Pf}}P_{1,0}$

Plainly for the data given in Table 1 and Table 2 these inequalities are satisfied.

We see from the system (5.1) that these two assumptions imply that the transport term between the two compartments and the elimination term are very small and may therefore be neglected. Thus, if we multiply the second equation by $D_{1,0}/P_{1,0}$ and add the result to the first equation we obtain to good approximation the conservation law

$$x_1(\tau_1) + \frac{D_{1,0}}{P_{1,0}}u_1(\tau_1) = \frac{D_{1,0}}{P_{1,0}} \tag{5.3}$$

which states that on this time scale no drug leaves the plasma compartment. Using (5.3) to eliminate x_1 from the second equation of (5.1), we end up with a single equation for u_1:

$$\frac{du_1}{d\tau_1} = f(u_1) \stackrel{\mathrm{def}}{=} (au_1 + 1)(1 - u_1) - a\frac{P_{1,0}}{D_{1,0}}u_1 \tag{5.4}$$

It is readily seen that $f(u_1)$ has a unique positive zero $\overline{u}_1$ and, using standard arguments from the theory of ordinary differential equations (Blanchard et al. (1998)), that

$$u_1(\tau_1) \to \overline{u}_1 \qquad \text{as} \qquad \tau_1 \to \infty \tag{5.5}$$

From the conservation law (5.3) we deduce that

$$\overline{x}_1(\tau_1) \to \overline{x}_1 \stackrel{\mathrm{def}}{=} \frac{D_{1,0}}{P_{1,0}}(1 - \overline{u}_1) \qquad \text{as} \qquad \tau_1 \to \infty \tag{5.6}$$

Thus, over a short interval u_1 and x_1 reach quasi-stationary "plateaus" at $\overline{u}_1$ and $\overline{x}_1$. These values will be referred to as *Plateau Values*. Some plateau values are presented in Table 3 below.

Table 3: Plateau values $\overline{u}_1$ and $\overline{x}_1$

K_P	0.1	1	10	100
$\overline{u}_1$	1.333×10^{-4}	1.331×10^{-3}	1.316×10^{-2}	1.176×10^{-1}
$\overline{x}_1$	1.333×10^{-4}	1.332×10^{-4}	1.316×10^{-4}	1.176×10^{-4}

Assumption 2: $D_{1,0} \ll P_{1,0}$.

Inspection of the function $f(u_1)$ in equation (5.4) shows that if $\delta = D_{1,0}/P_{1,0}$ is small, then $a\overline{u}_1 = O(\delta)$, so that we may put $a\overline{u}_1 + 1 \approx 1$ in (5.4) and conclude that

$$1 - \overline{u}_1 - a\frac{P_{1,0}}{D_{1,0}}\overline{u}_1 \approx 0$$

Since $aP_{1,0}/D_{1,0} = P_{1,0}/K_P$, we conclude that the plateau values $\overline{u}_1$ and $\overline{x}_1$ are well approximated by

$$\overline{u}_1 = \frac{\kappa_{P,1}}{1+\kappa_{P,1}} \qquad \text{and} \qquad \overline{x}_1 = \frac{D_{1,0}}{P_{1,0}}\frac{1}{1+\kappa_{P,1}} \qquad \text{where} \qquad \kappa_{P,1} = \frac{K_P}{P_{1,0}} \tag{5.7}$$

The half-time of the convergence towards the plateau values is then given by

$$\tau_{1,1/2} = \frac{\kappa_{P,1}}{1+\kappa_{P,1}}\ln 2 \tag{5.8}$$

Thus, the half-time ranges from about 10^{-4} sec (when $K_P = 0.1$) to 10^{-1} sec (when $K_P = 100$ μM).

For the larger times we scale time by the rate constant k_{Rb} and introduce the dimensionless time $\tau_2 = k_{\mathrm{Rb}}t$ (cf. eq. (4.8)). We now obtain the system

$$\begin{cases} \varepsilon\dfrac{dx_1}{d\tau_2} = +au_1 - (au_1+1)x_1, \\ \dfrac{du_1}{d\tau_2} = \dfrac{k_+}{k_{\mathrm{Rb}}}(u_2-u_1) + \dfrac{1}{\varepsilon}(au_1+1)\dfrac{P_{1,0}}{D_{1,0}}x_1 - \left(\dfrac{1}{\varepsilon}a\dfrac{P_{1,0}}{D_{1,0}} + \dfrac{k_{\mathrm{out}}}{k_{\mathrm{Rb}}}\right)u_1 \end{cases} \qquad \varepsilon = \frac{k_{\mathrm{Rb}}}{k_{\mathrm{Pb}}} \tag{5.9}$$

Assumption 3: $k_{\mathrm{Rb}} \ll k_{\mathrm{Pb}}$ so that $\varepsilon \ll 1$.

In light of this assumption, which is seen to be justified by the data, the system (5.9) is a singular perturbation problem. If we put $\varepsilon = 0$ in the first equation, we obtain

$$au_1 - (au_1+1)x_1 = 0 \qquad \Longrightarrow \qquad x_1 = \frac{au_1}{au_1+1} \tag{5.10}$$

Multiplying the first equation of (5.9) by $\varepsilon^{-1}(P_{1,0}/D_{1,0})$ and adding the result to the second equation yields

$$\frac{d}{d\tau_2}\left(u_1 + \frac{P_{1,0}}{D_{1,0}}x_1\right) = \frac{k_+}{k_{\mathrm{Rb}}}(u_2-u_1) - \frac{k_{\mathrm{out}}}{k_{\mathrm{Rb}}}u_1 \tag{5.11}$$

which is the dimensionless form of equation (4.3). Using (5.10) to eliminate x_1 from the left-hand side of (5.11) and writing

$$u_1 + \frac{P_{1,0}}{D_{1,0}}x_1 = u_1 + \frac{P_{1,0}}{D_{1,0}}\frac{au_1}{au_1+1} \stackrel{\text{def}}{=} \psi_1(u_1) \tag{5.12}$$

this equation can be written as

$$\psi_1'(u_1)\frac{du_1}{d\tau_2} = \frac{k_+}{k_{\rm Rb}}(u_2 - u_1) - \frac{k_{\rm out}}{k_{\rm Rb}}u_1 \tag{5.13}$$

where ψ_1' denotes the derivative of the function ψ_1.

Recall from (5.2) and (5.7) that $a\overline{u}_1 < (D_{1,0}/K_P)(K_P/P_{1,0}) = D_{1,0}/P_{1,0}$. Hence, by Assumption 2, $a\overline{u}_1 \ll 1$ so that, since $u_1 \le \overline{u}_1$, we can approximate ψ_1 and ψ_1' by

$$\tilde{\psi}_1(u_1) = u_1 + \frac{P_{1,0}}{D_{1,0}}au_1 = u_1 + \frac{P_{1,0}}{K_P}u_1 \quad \Longrightarrow \quad \tilde{\psi}_1'(u_1) = 1 + \frac{P_{1,0}}{K_P} = 1 + \frac{1}{\kappa_{P,1}} \tag{5.14}$$

Thus, equation (5.13) may be written as

$$\left(1 + \frac{1}{\kappa_{P,1}}\right)\frac{du_1}{d\tau_2} = \frac{k_+}{k_{\rm Rb}}(u_2 - u_1) - \frac{k_{\rm out}}{k_{\rm Rb}}u_1 \tag{5.15}$$

In light of the constants of Tables 1 and 2 we are justified in making the following assumption about the permeability of the membrane:

Assumption 4: $k_+ = PS/V_1 \ll k_{\rm out}$.

It follows that the exchange term $(k_+/k_{\rm Rb})(u_2 - u_1)$ is small compared to the elimination term $(k_{\rm out}/k_{\rm kRb})u_1$. This means that equation (5.15) may be approximated by the simpler equation

$$\left(1 + \frac{1}{\kappa_{P,1}}\right)\frac{du_1}{d\tau_2} = -\theta\, u_1, \qquad \theta = \frac{k_{\rm out}}{k_{\rm Rb}} \tag{5.16}$$

This equation can readily be solved explicitly. Taking as initial value the plateau value $\overline{u}_1$, right after the initial redistribution phase, we obtain the solution

$$u_1(\tau_2) = \overline{u}_1 e^{-(\kappa_{P,1}/(1+\kappa_{P,1}))\theta\,\tau_2} = \overline{u}_1 e^{-\alpha\, t} \tag{5.17}$$

where

$$\alpha = \frac{\kappa_{P,1}}{1 + \kappa_{P,1}}\, k_{\rm out} \tag{5.18}$$

If $K_P \le 10$, then $\kappa_P \le 1/75 = 0.0133$, i.e., $\kappa_P \ll 1$, so that, approximately,

$$\alpha = \kappa_{P,1}\, k_{\rm out} \tag{5.19}$$

Remark. We conclude from the expression (5.17) that to good approximation, the free drug concentration in the plasma compartment is unaffected by processes in the brain compartment.

6 Dynamics in the brain compartment

Since the influx of drug into the brain compartment is negligible during the short time equilibration of the drug and the protein in the plasma compartment, we focus here on the

longer time scale. For the three complexes we obtain the following system of equations

$$\begin{cases} \varepsilon \dfrac{dx_2}{d\tau_2} = +au_2 - (au_2+1)x_2 \\ \dfrac{dy_2}{d\tau_2} = +bu_2 - (bu_2+1)y_2 \\ \mu \dfrac{dz_2}{d\tau_2} = +cu_2 - (cu_2+1)z_2 \end{cases} \tag{6.1}$$

where

$$a = \frac{k_{\mathrm{Pf}}}{k_{\mathrm{Pb}}} D_{1,0}, \qquad b = \frac{k_{\mathrm{Rf}}}{k_{\mathrm{Rb}}} D_{1,0}, \qquad c = \frac{k_{\mathrm{Lf}}}{k_{\mathrm{Lb}}} D_{1,0}, \qquad \varepsilon = \frac{k_{\mathrm{Rb}}}{k_{\mathrm{Pb}}}, \qquad \mu = \frac{k_{\mathrm{Rb}}}{k_{\mathrm{Lb}}} \tag{6.2}$$

Assumption 5: $k_{\mathrm{Rb}} \ll k_{\mathrm{Lb}}$ so that $\mu \ll 1$.

Substituting the data listed in Tables 1 and 2, these constants have the following values:

$$a = 10^2 - 10^{-1}, \qquad b = 10^4, \qquad c = 1, \qquad \varepsilon = 10^{-2} - 10^{-5}, \qquad \mu = (2-50)\times 10^{-5} \tag{6.3}$$

when $k_{\mathrm{Pb}} = 1000$, 100, 10 and 1 and $k_{\mathrm{Lb}} = 500$, 100 and 20. For the drug we have

$$\begin{aligned} \frac{du_2}{d\tau_2} = \frac{k_-}{k_{\mathrm{Rb}}}(u_1 - u_2) + \frac{1}{\varepsilon}(au_2+1)\frac{P_{2,0}}{D_{1,0}}x_2 + (bu_2+1)\frac{R_{2,0}}{D_{1,0}}y_2 \\ + \frac{1}{\mu}(cu_2+1)\frac{L_{2,0}}{D_{1,0}}z_2 - \left(\frac{1}{\varepsilon}a\frac{P_{2,0}}{D_{1,0}} + b\frac{R_{2,0}}{D_{1,0}} + \frac{1}{\mu}c\frac{L_{2,0}}{D_{1,0}}\right)u_2 \end{aligned} \tag{6.4}$$

We now multiply the first equation of the system (6.1) by $P_{2,0}/(\varepsilon D_{1,0})$ and the third equation by $L_{2,0}/(\mu D_{1,0})$ and then add these equations to the drug equation (6.4). This then yields

$$\frac{d}{d\tau_2}\left(u_2 + \frac{P_{2,0}}{D_{1,0}}x_2 + \frac{L_{2,0}}{D_{1,0}}z_2\right) = \frac{k_-}{k_{\mathrm{Rb}}}(u_1 - u_2) + (bu_2+1)\frac{R_{2,0}}{D_{1,0}}y_2 - b\frac{R_{2,0}}{D_{1,0}}u_2 \tag{6.5}$$

Since ε and μ are small, the system consisting of (6.1) and (6.4) constitutes again a singular perturbation problem and to first approximation we may put

$$x_2 = \frac{au_2}{au_2+1} \qquad \text{and} \qquad z_2 = \frac{cu_2}{cu_2+1} \tag{6.6}$$

The initial conditions satisfy these relations and we may therefore assume that (6.6) holds for all time. Thus, we can eliminate x_2 and z_2 from equation (6.5) so that the first term only involves the drug concentration in the brain, u_2:

$$u_2 + \frac{P_{2,0}}{D_{1,0}}x_2 + \frac{L_{2,0}}{D_{1,0}}z_2 = u_2 + \frac{P_{2,0}}{D_{1,0}}\frac{au_2}{au_2+1} + \frac{L_{2,0}}{D_{1,0}}\frac{cu_2}{cu_2+1} \stackrel{\text{def}}{=} \psi_2(u_2) \tag{6.7}$$

Equation (6.5) can now be rewritten as

$$\psi_2'(u_2)\frac{du_2}{d\tau_2} = \frac{k_-}{k_{\mathrm{Rb}}}(u_1 - u_2) + (bu_2+1)\frac{R_{2,0}}{D_{1,0}}y_2 - b\frac{R_{2,0}}{D_{1,0}}u_2 \tag{6.8}$$

where ψ_2' denotes the derivative of the function ψ_2.

Observe that

$$au_2 = \frac{D_{1,0}}{K_P}u_2 < \frac{D_{1,0}}{K_P}\overline{u}_1 < \frac{D_{1,0}}{K_P}\kappa_{P,1} = \frac{D_{1,0}}{P_{1,0}} \ll 1$$

where we have used the approximate expression for $\overline{u}_1$ given in (5.7) and Assumption 2. Similarly, we find that

$$cu_2 = \frac{D_{1,0}}{K_L}u_2 < \frac{D_{1,0}}{K_L}\overline{u}_1 < \frac{D_{1,0}}{K_L}\kappa_{P,1} = \frac{D_{1,0}}{P_{1,0}}\frac{K_P}{K_L} \ll 1$$

Therefore, we may ignore these terms in the denominators in (6.7) and replace the non-linear function $\psi_2(u)$ by a linear function:

$$\tilde{\psi}_2(u) = u + \frac{P_{2,0}}{K_P}u + \frac{L_{2,0}}{K_L}u \qquad \Longrightarrow \qquad \tilde{\psi}_2'(u) = 1 + \frac{P_{2,0}}{K_P} + \frac{L_{2,0}}{K_L}$$

Thus, we are justified in simplifying the system (6.1), (6.8) to

$$\begin{cases} \dfrac{dy_2}{d\tau_2} = bu_2 - (bu_2+1)y_2 \\ \dfrac{1}{\kappa_{m,2}}\dfrac{du_2}{d\tau_2} = \dfrac{k_-}{k_{\mathrm{Rb}}}(u_1-u_2) + \dfrac{R_{2,0}}{D_{1,0}}\{y_2(bu_2+1) - bu_2\} \end{cases} \tag{6.9}$$

where we have written

$$\kappa_{m,2} = \left(1 + \frac{P_{2,0}}{K_P} + \frac{L_{2,0}}{K_L}\right)^{-1} \tag{6.10}$$

This system can be solved explicitly. However, for the range of parameter values studied in this paper, it is possible to make one further simplification.

Transforming to the new time variable

$$\tau_3 = \kappa_{m,2}\tau_2 = \kappa_{m,2}k_{\mathrm{Rb}}t \tag{6.11}$$

we can write the system (6.9) as

$$\begin{cases} \kappa_{m,2}\dfrac{dy_2}{d\tau_3} = bu_2 - (bu_2+1)y_2 \\ \dfrac{du_2}{d\tau_3} = \dfrac{k_-}{k_{\mathrm{Rb}}}(u_1-u_2) + \dfrac{R_{2,0}}{D_{1,0}}\{y_2(bu_2+1) - bu_2\} \end{cases} \tag{6.12}$$

In light of our parameter values, the following assumption is justified:

Assumption 6: $K_L \ll L_{2,0}$.

Invoking this assumption, we conclude that $\kappa_{m,2} < \kappa_{L,2} \ll 1$ and hence, that we may assume that drug and receptor are in quasi-equilibrium, i.e., to good approximation we have

$$bu_2 - (bu_2+1)y_2 = 0 \qquad \Longrightarrow \qquad y_2 = \frac{bu_2}{bu_2+1} \tag{6.13}$$

Using this identity in the second equation of (6.11), and observing that k_-/k_{Rb} and $R_{2,0}/D_{1,0}$ have the same order of magnitude, we are left with the single equation

$$\frac{du_2}{d\tau_3} = \frac{k_-}{k_{\mathrm{Rb}}}(u_1 - u_2). \tag{6.14}$$

Remembering that $u_1(t)$ is well approximated by the exponential function given in (5.17) we can approximate (6.14) by

$$\frac{du_2}{dt} = \beta\left(\overline{u}_1 e^{-\alpha t} - u_2\right), \qquad \alpha = \frac{\kappa_{P,1}}{\kappa_{P,1}+1}\, k_{\mathrm{out}}, \qquad \beta = \kappa_{m,2} k_- \tag{6.15}$$

where we have returned to the original time variable t using (5.17) and (6.11). Equation (6.15) can be solved explicitly. Since $u_2(0) = 0$ we obtain

$$u_2(t) = \frac{\beta}{\beta - \alpha}\overline{u}_1\left(e^{-\alpha t} - e^{-\beta t}\right). \tag{6.16}$$

In Figure 7 we show graphs of $D_1(t)$ (dashed) and $D_2(t)$ (solid) computed numerically (in blue) as well as graphs of the approximations of the drug concentrations presented in (5.17) and (6.16) (in red) for $K_P = 0.1$, 1 and 10, and $K_L = 10$. Evidently, for these affinities the correspondence between numerical graphs and analytical approximations is excellent, confirming analytical predictions.

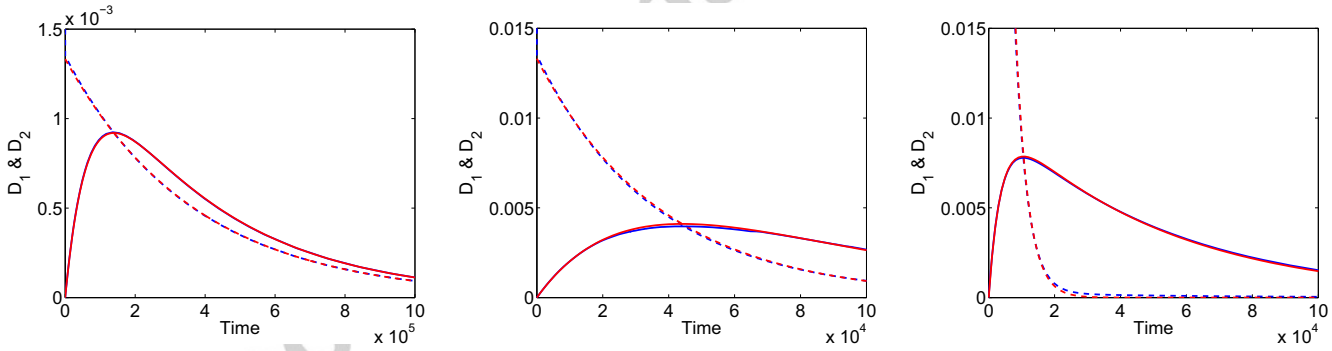

$K_P = 0.1$ $K_P = 1$ $K_P = 10$

Figure 7: Graphs of the solutions $D_1(t)$ (dashed) and $D_2(t)$ (solid) of the system (4.1), (4.2) (in blue) computed numerically, as well as graphs of the corresponding approximate concentration profiles given by (5.17) and (6.16) (in red) with rate constants given in Table 1 for $K_P = 0.1$, 1 and 10 ($k_{\mathrm{Pb}} = 1, 10, 100$), and $K_L = 10$. Initial concentrations are given in Table 2. Note that, while the scale of the figures for K_P=1 and 10 is the same, in the figure for K_P=0.1, the horizontal scale had been shrunk by a factor 10 and the vertical scale has been blown up by a factor 10. Time in seconds.

We conclude from (6.16) that the terminal slope $\lambda_{z,1}$ of u_1 is always α and the terminal slope $\lambda_{z,2}$ of u_2 is either α or β, depending on which is the smallest. Thus:

• If $\alpha < \beta$, i.e., when $\kappa_{P,1} k_{\text{out}} < \kappa_{m,2} PS/V_2$, e.g. when the drug has high affinity to the proteins and $K_P \ll P+1, 0$, then the terminal slopes $\lambda_{z,1}$ and $\lambda_{z,2}$ in the two compartments are given by

$$\lambda_{z,1} = \lambda_{z,2} = \alpha = \kappa_{P,1} k_{\text{out}} \tag{6.17}$$

• If $\alpha > \beta$, i.e., when $\kappa_{P,1} k_{\text{out}} > \kappa_{m,2} PS/V_2$, e.g. when the drug has high affinity to the lipids, or the permeability of the membrane is small, then the terminal slopes are given by

$$\lambda_{z,1} = \alpha \qquad \text{and} \qquad \lambda_{z,2} = \beta = \kappa_{m,2} \frac{PS}{V_2} \tag{6.18}$$

In Figure 7 we see these properties demonstrated: for $K_P = 1$, the rate constants of Table 1 and the concentrations of Table 2 we have $\alpha = 2.67 \times 10^{-5}$ and $\beta = 1.91 \times 10^{-5}$, i.e. $\alpha \approx \beta$. Therefore, when $K_P = 0.1$ then $\alpha < \beta$ and the elimination rates of u_1 and u_2 are the same, and when $K_P = 10$ then $\alpha > \beta$ and (6.18) applies and u_2 decays much more slowly than u_1.

7 Receptor occupancy

As is well known (see also PBG), receptor occupancy $DR_2/R_{2,0}$ is an important determinant in assessing the effectiveness of a drug. In this section we analyse this quantity and the way it depends on different parameters.

The previous analysis has yielded an important tool for the study of the receptor occupancy: we have seen that for the parameter ranges involved drug and receptor are rapidly in quasi-equilibrium and that

$$\frac{DR_2(t)}{R_{2,0}} = \frac{D_2(t)}{D_2(t) + K_R} \quad \text{or} \qquad y_2(t) = \frac{b u_2(t)}{b u_2(t) + 1}, \qquad b = \frac{D_{1,0}}{K_R} \tag{7.1}$$

where $u_2(t)$ is the dimensionless drug concentration in the brain compartment. Having obtained accurate analytical approximations for $u_2(t)$, equation (7.1) yields an analytical approximation for $DR_2(t)$ and the receptor occupancy $y_2(t)$, and hence it is now possible to approach the question as to the impact of different parameters also from an analytical perspective.

In Figure 8 we first present a series of numerically computed graphs of $DR_2(t)$ for different values of K_P and K_L, as they were shown in Figure 2. To demonstrate the accuracy of the analytic approximations for $DR_2(t)$, these have been included (the dashed curves).

The analytical approximation of $DR_2(t)$ now enables us to interpret these simulations, both qualitatively and quantitatively. We discuss the two figures separately.

Impact of K_P (left): Here we fixed $K_L = 10$ and let K_P take an increasing series of values. We first compare this figure with a comparable one in PBG where the one-compartment system without lipids was analysed. We find that here the half-life of $DR_2(t)$ remains much larger than we observed in the one-compartment system. In that setting the half-life becomes quite small as $K_P \to 100$.

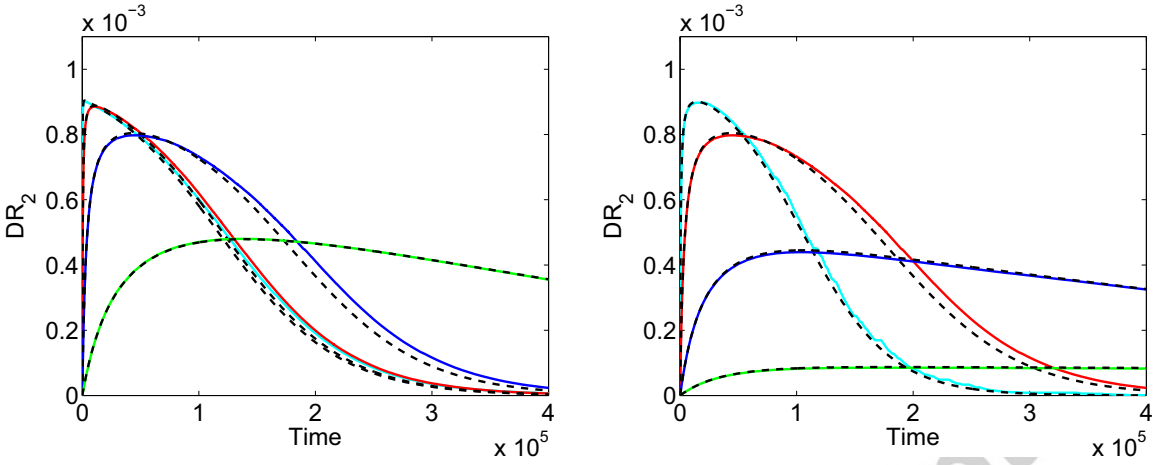

$K_P = 100, 10, 1, 0.1$ & $K_L = 10$ $\qquad$ $K_L = 100, 10, 1, 0.1$ & $K_P = 1$

Figure 8: Graphs of $DR_2(t)$ of the system (2.7) - (2.11) over a period of about 110 hours. On the left: k_{Pb} ranges from 1000 (acqua), 100 (red), 10 (blue), 1 (green), and on the right k_{Lb} ranges from 1000 (acqua), 100 (red), 10 (blue), 1 (green). The other rate constants are taken from Table 1; initial concentrations are given by Table 2. The black dashed curves are the corresponding analytical approximations based on the expressions (7.1) and (6.16). Note that the blue curve in the figure on the left and the red curve in the one on right are the same. Time in seconds.

The analysis in the previous section shows how - and to what extent - the division into two compartments and the presence of the lipids in the brain compartment has this effect. As K_P increases, the elimination rate in the plasma compartment α increases and eventually overtakes β. When this happens, β becomes the elimination rate for the brain compartment. If $\lambda_{z,2}$ is the terminal slope of u_2, and hence of y_2 or DR_2, then for K_P large enough, $\lambda_{z,2} = \beta$. If in addition $K_L \ll L_{2,0}$, then $\kappa_{m,2} \approx \kappa_{L,2}$, and hence, by (6.18),

$$\lambda_{z,2} = \beta \approx \frac{K_L}{L_{2,0}} \frac{PS}{V_2} \approx 2K_L \times 10^{-6} \tag{7.2}$$

where we have used data from Tables 1 and 2. Thus, for $K_L = 10$ we have $\lambda_{z,2} \approx 2 \times 10^{-5}$, which yields a half-time of 3.5×10^4 sec. This value is consistent with the half-time shown in Figures 2 and 8 (left).

Impact of $\mathbf{K_L}$ (right): In this figure we fixed $K_P = 1$ and let K_L decrease from 100 to 0.1. Thus, here α is fixed ($\alpha = 2.7 \times 10^{-5}$) and by (6.9), the value of β decreases. In addition, when $\kappa_{L,2} = K_L/L_{2,0} \ll 1$, then β is given by (7.2). Thus, once K_L is small enough, then $\beta < \alpha$ and hence the terminal slope is given by β and hence proportional to K_L. Hence, when K_L is reduced by factors of 10, then at each reduction the half-time increases by a factor of 10. These properties are plainly evident in the right-hand set of graphs in Figure 8.

Impact of $\mathbf{k_{out}}$: Naturally, the elimination rate k_{out} is closely connected to the elimination rate α of the plasma compartment. In the left graphs in Figure 9 we show how when k_{out}

is increased by a factor 10, i.e., we put $k_{\text{out}} = 0.2$, the maximum value of DR_2 drops by about a factor 2. However, reducing the off-rate k_{Rb} by a factor 10 – and hence K_R also by a factor 10 – brings the receptor occupancy back up to levels of around 80 %. This can be explained by inspecting the explicit approximation of $u_2(t)$. By increasing k_{out} and hence α we see that $u_2(t)$ becomes smaller and hence, so does $y_2(t)$ (for all the values of K_P we have $\alpha > \beta$, cf. Table 4). From the expression (7.1) we see that reducing K_R has the effect of raising the receptor occupancy.

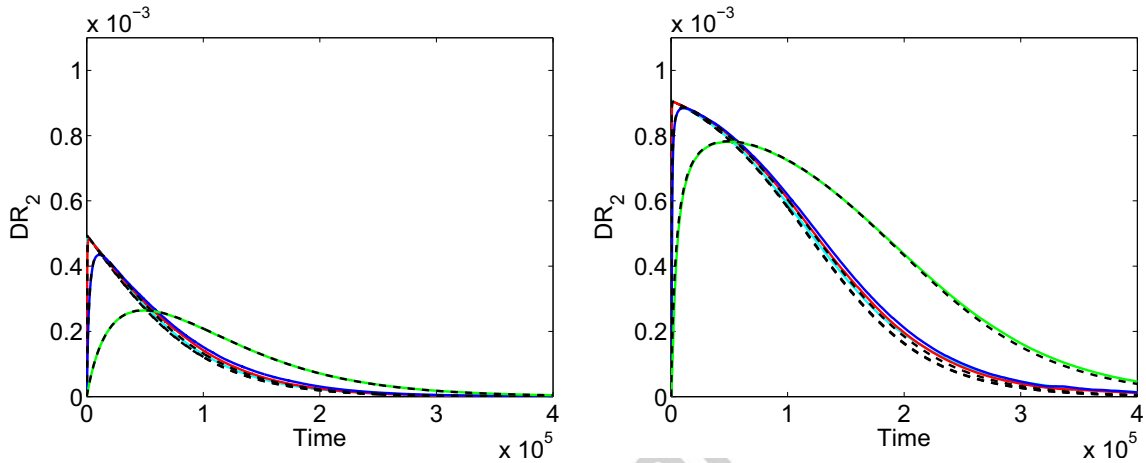

$k_{\text{Rb}} = 0.01$ $k_{\text{Rb}} = 0.001$

Figure 9: Graphs of DR_2 versus time over ± 110 hours – both numerical (solid) and analytical (dashed) – for $K_P = 0.1$, 1, 10 and 100 for $k_{\text{out}} = 0.2$ and for $k_{\text{Rf}} = 10$, $k_{\text{Rb}} = 0.01$ and 0.001, so that $K_R = 10^{-3}$ and 10^{-4}, $K_L = 10$ and $D_{1,0} = 10$. Time in seconds.

The dashed curves in Figure 9 have been computed by means of the explicit expression for $u_2(t)$. They demonstrate the accuracy with which these approximate analytical expressions predict the complex behaviour of the system.

Area under the receptor occupancy curve AUCRO: In accord with our earlier analysis of a one-compartment model (PBG) and for reasons of simplicity and transparency, we have used the area under the curve for receptor occupancy ($AUCRO$) as a summary measure of pharmacology, i.e. we estimate the integral

$$AUCRO(K_P, K_L) = \int_0^T \frac{DR_2(t)}{R_{2,0}} dt \tag{7.3}$$

in which T denotes an appropriate time horizon, and we discuss the manner in which this quantity is impacted by the affinities K_P and K_L.

This assumes that the $AUCRO$ is proportional to pharmacological effect, which although generally thought to be true and supported by some data, for example, see Jusko (1995), it should be interpreted with the caveat that some exceptions to this may exist.

In Figure 10 we use the approximation (6.16) for the concentration of free drug in the brain to explore how the area under the receptor-occupancy curve over a clinically

common period of 24 h depends on K_P and K_L. Remembering that $y_2(t)$ denotes the dimensionless receptor occupancy we consider the function

$$AUCRO(K_P, K_L) = \int_0^T y_2(t)\, dt = \int_0^T \frac{bu_2(t)}{bu_2(t)+1}\, dt, \qquad T = 24 \text{ h} = 86400 \text{ sec} \quad (7.4)$$

and we show how it changes as K_P varies from 0 to 4. We do this for two values of the affinity K_L of the drug to the lipids. Notice the qualitative difference between the

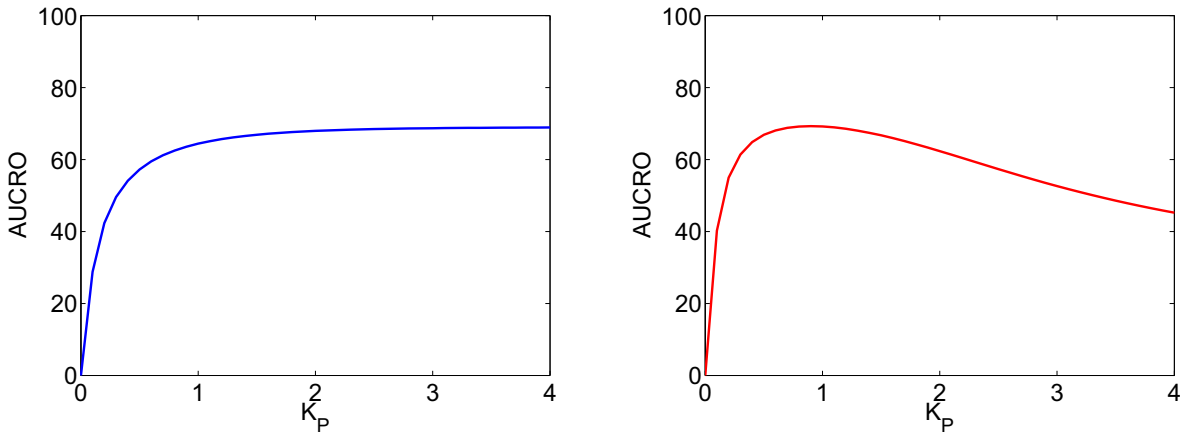

$K_L = 10$ $K_L = 100$

Figure 10: Graphs of the $AUCRO$ over 24 hours, versus $K_P \in (0, 4]$ for $K_L = 10$ and 100, computed with the approximation (6.16) for the dimensionless drug concentration $u_2(t)$ in the brain compartment used in the expression for $y_2(t)$ given in (7.1). Data are taken from Tables 1 and 2.

two graphs. The one on the left, for $K_L = 10$, is increasing for all $0 < K_P \leq 4$, whilst the one on the right, for $K_L = 100$, has a maximum - the *Sweet Spot* - for $K_P \approx 1$. Thus, evidently when K_L is large enough there exists a unique value for K_P for which the receptor occupancy in the brain is maximal.

The impact of the permeability surface area product PS runs parallel with the affinity of the drug to the lipids. This is best seen from the expression for the terminal slope $\lambda_{z,2}$ given in equation (7.2), which is valid when $K_L \ll L_{2,0}$. There K_L and PS appear as a product. As we have seen in (6.18), when PS becomes small, then β becomes small and the terminal slope of the system will be given by β. When K_L is also small then β will be given by (7.2) and we may conclude that changes in PS and in K_L have an identical impact.

8 Constant rate drug infusion into the plasma

The analysis developed for the model described in Section 2 can be applied to a wide range of related models. In this section we change the mode of administration and focus on two such models involving a constant rate infusion into the plasma compartment. If

we denote the amount of drug supplied per second by In, then this leads to an additional zeroth order term $k_{\text{infus}} = In/V_1$ in the equation for the free drug concentration in the plasma compartment.

Apart from the infusion term, the first model discussed in this section is the same as that discussed in the previous sections. In the second model we include an additional route along which free drug flows from the brain to the plasma compartment.

8.1 No drug elimination from the brain

The model analysed in this subsection is the same as that discussed in Sections 2-7, except that free drug now flows at a constant rate into the plasma compartment. Thus the model equations remain the same, except for the equation for the drug concentration in the plasma compartment, which now includes a the zeroth order infusion term k_{infus}:

$$\frac{dD_1}{dt} = k_{\text{infus}} + k_+(D_2 - D_1) - k_{\text{Pf}} D_1 \cdot P_1 + k_{\text{Pb}} D P_1 - k_{\text{out}} D_1 \tag{8.1}$$

We assume that at the time ($t = 0$), when the infusion starts, the system is free of drug, i.e. $D_1(0) = 0$, $D_2(0) = 0$, and all the initial values of the drug complexes are zero too.

Inspection of the system (4.1), (4.2) modified accordingly, readily shows that the steady state drug concentration in the two compartments is the same, i.e., at equilibrium,

$$D_1 = D_2 = D_{\text{ss}} \stackrel{\text{def}}{=} \frac{k_{\text{infus}}}{k_{\text{out}}} \qquad \text{and} \qquad DR_{2,\text{ss}} = R_{2,0}\frac{D_{\text{ss}}}{D_{\text{ss}} + K_R} \tag{8.2}$$

We make the equations dimensionless, using D_{ss} as a reference value for the drug concentrations in the two compartments, i.e., $u_i(t) = D_i(t)/D_{\text{ss}}$ ($i = 1, 2$), and keep the other reference concentrations the same. When the rate of infusion is small enough so that $D_{\text{ss}} \ll K_P$ and hence $D_i(t) \ll K_P$, as was the case in Sections 5 and 6, we can reproduce the arguments employed in these sections to obtain the following system of equations:

$$\begin{cases} \dfrac{1}{\kappa_{P,1}}\dfrac{du_1}{d\tau_2} = \dfrac{k_{\text{infus}}}{k_{\text{Rb}} D_{\text{ss}}} + \dfrac{k_+}{k_{\text{Rb}}}(u_2 - u_1) - \dfrac{k_{\text{out}}}{k_{\text{Rb}}}u_1 \\ \dfrac{1}{\kappa_{m,2}}\dfrac{du_2}{d\tau_2} = \dfrac{k_-}{k_{\text{Rb}}}(u_1 - u_2) \end{cases} \tag{8.3}$$

This system is comparable to the differential equations (5.15) and (6.14) for respectively u_1 and u_2. Returning to the original time variable, we arrive at

$$\begin{cases} \dfrac{1}{\kappa_{P,1}}\dfrac{du_1}{dt} = k_{\text{out}}(1 - u_1) + k_+(u_2 - u_1) \\ \dfrac{1}{\kappa_{m,2}}\dfrac{du_2}{dt} = k_-(u_1 - u_2) \end{cases} \tag{8.4}$$

As in Section 6, we utilise the fact that $k_+ \ll k_{\text{out}}$ and neglect the drug loss from the plasma to the brain in the first of the two equations of (8.4). This modification of the first equation in (8.4) yields an equation involving $u_1(t)$ only, which can be solved explicitly. Since $u_1(0) = 0$, we obtain

$$u_1(t) = 1 - e^{-\alpha t}, \qquad \alpha = \kappa_{P,1} k_{\text{out}} \tag{8.5}$$

Substituting this expression into the second equation of (8.4) yields an equation involving only $u_2(t)$:

$$\frac{du_2}{dt} = \beta\left(1 - e^{-\alpha t} - u_2\right), \qquad \beta = \kappa_{m,2}k_- \tag{8.6}$$

For the solution u_2 of equation (8.6) which satisfies the initial condition $u_2(0) = 0$, we find

$$u_2(t) = 1 - \frac{\beta}{\beta - \alpha}e^{-\alpha t} + \frac{\alpha}{\beta - \alpha}e^{-\beta t} \qquad (\beta \neq \alpha) \tag{8.7}$$

In Figure 11 we show graphs of numerical solutions of the system (2.7) - (2.11), where the equation for dD_1/dt has been replaced by (8.1), and compare them with the corresponding graphs of $D_{\rm ss}u_1(t)$ and $D_{\rm ss}u_2(t)$, where $u_1(t)$ and $u_2(t)$ are the analytical approximations of the free drug concentrations given by, respectively, (8.5) and (8.7). It is clear that for $K_P = 10$, 1 and 0.1, the numerical and the analytic curves are very close.

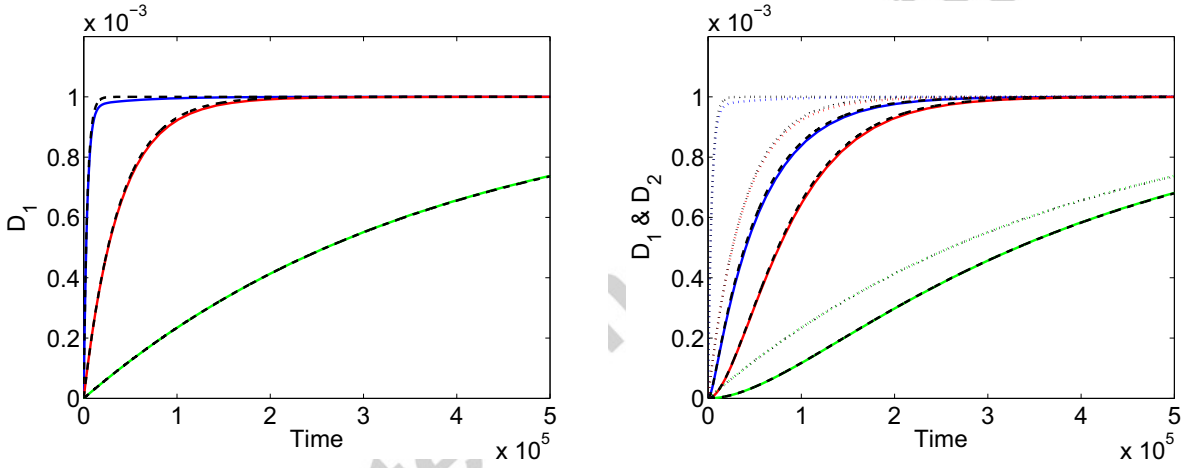

Figure 11: Graphs of $D_1(t)$ (left) and $D_2(t)$ (right) over $\pm$ 140 hours of the system (2.7) - (2.11) modified to include a constant rate infusion $k_{\rm infus} = 0.00002$ (cf. (8.4)), so that $D_{\rm ss} = 0.001$, for $k_{\rm Pb} = 1000$ (aqua), 100 (blue), 10 (red) and 1 (green) and $K_L = 10$. The solid curves are computed numerically and the dashed curves are the corresponding graphs of the function $D_{\rm ss}u_1(t)$ where $u_1(t)$ is given by the formula (8.5) and $D_{\rm ss}u_2(t)$ where $u_2(t)$ is given by the formula (8.7). In the figure on the right the dotted curves are the curves associated with $D_1(t)$ shown in the figure on the left. Time in seconds.

In Figure 12 we show how the ratio of the free drug concentration in the brain compartment over the free drug concentration in the plasma varies with time and with the dissociation constant K_P of the drug and the proteins. We use the analytical expressions obtained for $u_1(t)$ and $u_2(t)$ since we have seen that they provide good approximations to the real concentrations.

Consistent with the observation (8.2) that at equilibrium the two concentrations are the same, we observe that $D_2(t)/D_1(t) \to 1$ as $t \to \infty$ with a rate which depends on K_P. The impact of K_P is felt through the value of $\alpha = \kappa_{P,1}k_{\rm out}$ and, since the amount of proteins in the brain compartment is much smaller than in the plasma compartment, to

a much smaller extent also through the value of β. In Table 4 we have listed the values of α and β for the values of the rate constants pertaining to the graphs in Figure 12.

Table 4: Values of α and β when $K_L = 10$ μM

K_P	10	1	0.1
α	2.67×10^{-4}	2.6×10^{-5}	2.6×10^{-6}
β	1.95×10^{-7}	1.91×10^{-7}	1.51×10^{-7}

As K_P decreases, the drug has a greater tendency to be bound to the proteins and it therefore takes longer to be released. Thus $D_1(t)$ decays, more slowly, as we also see back in the expression for $u_1(t)$. In the brain compartment, the drug concentration is dominated by the lipid binding which does not change. Therefore, we see that as K_P decreases, the quotient D_2/D_1 drops and takes longer to reach the limiting value 1.

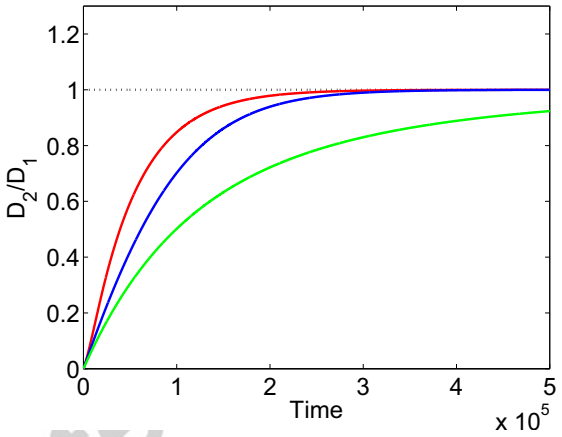

Figure 12: Graphs of $D_2(t)/D_1(t)$ of the system (2.7) - (2.11) (over $\pm$ 140 h), modified to include a constant rate infusion $k_{\text{infus}} = 0.00002$, so that $D_{\text{ss}} = 0.001$, for $k_{\text{Pb}} = 100$ (blue), 10 (red) and 1 (green) and $K_L = 10$. The curves are computed analytically using the expressions (8.5) and (8.7) for, respectively, $u_1(t)$ and $u_2(t)$. Time in seconds.

8.2 Drug flow from the brain to the plasma

In the system studied in the previous subsection drug could only leave the brain compartment though the blood-brain barrier. In reality, it is known that drug can also leave the brain compartment through a different route: flowing convectively into a sub-compartment containing the *Cerebrospinal fluid* (CSF) and from there into the plasma. Its volume is about 100 ml (cf. Grant et al. (1989)). The CSF-compartment empties though a different route into the plasma-compartment.

Transfer to the CSF-compartment is very fast, so that there is no need to treat it as a separate compartment. In normal humans the CSF turns over about every six hours (cf. Silverberga et al. (2003)) and hence a half-time of about 1h can be estimated yielding a

rate constant $k_{\rm CSF}$ of about 0.7 $\rm h^{-1}$. Since the CSF volume is estimated at 0.1 L, this yields a clearance of $k_{\rm CSF} \times 0.1 = 0.07$ L/h.

In this sub-section we study a modification of the system discussed in the previous subsection in which we incorporate this drug route from the brain into the plasma by a simple linear elimination term from the brain. For the sake of transparency, we first write the two-compartment system for the free drug alone, assuming there are no proteins, lipids and receptors in either compartment. This yields:

$$\begin{cases} V_1 \dfrac{dD_1}{dt} = In + PS(D_2 - D_1) - k_{\rm out} V_1 D_1 + Cl \cdot D_2 \\ V_2 \dfrac{dD_2}{dt} = -PS(D_2 - D_1) - Cl \cdot D_2 \end{cases} \tag{8.8}$$

Here Cl denotes the *Clearance* of the drug from the brain compartment along the new route. It appears in the equation for dD_2/dt as a loss term and, since this route discharges into the plasma, in the equation for dD_1/dt as a growth term. When we write

$$k_{\rm infus} = \frac{\rm In}{V_1}, \qquad k_+ = \frac{PS}{V_1}, \qquad k_- = \frac{PS}{V_2}, \qquad k_{\rm p} = \frac{Cl}{V_1}, \qquad k_{\rm b} = \frac{Cl}{V_2} \tag{8.9}$$

and put back the proteins, the lipids and the receptors, we end up with the following modification of the system (2.11):

$$\begin{cases} \dfrac{dD_1}{dt} = k_{\rm infus} + k_+(D_2 - D_1) - k_{\rm Pf} D_1 \cdot P_1 + k_{\rm Pb} DP_1 - k_{\rm out} D_1 + k_{\rm p} D_2 \\ \dfrac{dD_2}{dt} = -k_-(D_2 - D_1) - k_{\rm Pf} D_2 \cdot P_2 + k_{\rm Pb} DP_2 \\ \qquad\qquad - k_{\rm Rf} D_2 \cdot R_2 + k_{\rm Rb} DR_2 - k_{\rm Lf} D_2 \cdot L_2 + k_{\rm Lb} DL_2 - k_{\rm b} D_2 \end{cases} \tag{8.10}$$

Note that the steady state drug concentrations are

$$D_{1,\rm ss} = \frac{\rm In}{k_{\rm out} V_1} = \frac{k_{\rm infus}}{k_{\rm out}}, \qquad D_{2,\rm ss} = \frac{PS}{PS + Cl} D_{1,\rm ss} = \frac{PS}{PS + Cl} \frac{\rm k_{infus}}{k_{\rm out}} \tag{8.11}$$

i.e., in contrast to the previous model, they are now different. In particular

$$\frac{D_{2,\rm ss}}{D_{1,\rm ss}} = \frac{PS}{PS + Cl} \stackrel{\rm def}{=} \Lambda \tag{8.12}$$

which reverts to 1 when $Cl = 0$, as in the previous model.

As in our previous analyses, we make the equations dimensionless. This time we use $D_{\rm ss,1}$ as a reference value for the drug concentrations in the two compartments, i.e., $u_i(t) = D_i(t)/D_{\rm ss,1}$ $(i = 1, 2)$. The other reference concentrations are kept the same. When the rate of infusion is small enough so that $D_{\rm ss,1} \ll K_P$ and hence $D_i(t) \ll K_P$, as was the case in Sections 5 and 6, we can reproduce the arguments employed in these sections to obtain the following system of equations:

$$\begin{cases} \dfrac{1}{\kappa_{P,1}} \dfrac{du_1}{d\tau_2} = \dfrac{k_{\rm infus}}{k_{\rm Rb} D_{\rm ss,1}} + \dfrac{k_+}{k_{\rm Rb}}(u_2 - u_1) - \dfrac{k_{\rm out}}{k_{\rm Rb}} u_1 + \dfrac{k_{\rm p}}{k_{\rm Rb}} D_2 \\ \dfrac{1}{\kappa_{m,2}} \dfrac{du_2}{d\tau_2} = \dfrac{k_-}{k_{\rm Rb}}(u_1 - u_2) - \dfrac{k_{\rm b}}{k_{\rm Rb}} D_2 \end{cases} \tag{8.13}$$

As in Subsection 8.1, this system is comparable to the differential equations (5.15) and (6.14) for respectively u_1 and u_2. Returning to the original time variable, we arrive at

$$\begin{cases} \dfrac{1}{\kappa_{P,1}}\dfrac{du_1}{dt} = k_{\rm out}(1-u_1) + k_+(u_2-u_1) + k_{\rm p}u_2 \\ \dfrac{1}{\kappa_{m,2}}\dfrac{du_2}{dt} = k_-(u_1-u_2) - k_{\rm b}u_2 \end{cases} \tag{8.14}$$

Plainly, the steady state values of u_1 and u_2 are now

$$u_{\rm ss,1} = 1 \qquad \text{and} \qquad u_{\rm ss,2} = \frac{PS}{PS+Cl} \tag{8.15}$$

As we explained above, a common value for Cl is 0.07 L/h, which is small compared to the value of PS of 10 L/h, given in Table 1. Therefore, in the equation for du_1/dt the second and the third term on the right are small, and we may approximate it by

$$\frac{1}{\kappa_{P,1}}\frac{du_1}{dt} = k_{\rm out}(1-u_1) \tag{8.16}$$

Its solution $u_1(t)$, that starts at zero, i.e., for which $u_1(0) = 0$, is given by

$$u_1(t) = 1 - e^{-\alpha t}, \qquad \alpha = \kappa_{P,1}k_{\rm out} \tag{8.17}$$

Substitution into the second equation of (8.14) yields

$$\frac{du_2}{dt} = \beta(1-e^{-\alpha t}) - (\beta+\gamma)u_2, \qquad \beta = \kappa_{m,2}k_-, \quad \gamma = \kappa_{m,2}k_{\rm b} \tag{8.18}$$

The solution $u_2(t)$ of this equation, which starts at zero is given by

$$u_2(t) = \frac{\beta}{\beta+\gamma} - \frac{\beta}{\beta+\gamma-\alpha}e^{-\alpha t} + \frac{\alpha\beta}{(\beta+\gamma)(\beta+\gamma-\alpha)}e^{-(\beta+\gamma)t} \tag{8.19}$$

Plainly,

$$\frac{u_2(t)}{u_1(t)} \to \frac{\beta}{\beta+\gamma} = \frac{PS}{PS+Cl} \qquad \text{as} \qquad t\to\infty \tag{8.20}$$

In Figure 13 we show the graphs of the drug concentrations $D_1(t)$ and $D_2(t)$ in the two compartments (left) as well as graphs of the quotient $D_2(t)/D_1(t) = u_2(t)/u_1(t)$ for this model when PS takes on the values 10, 1, 0.1, 0.01 L/h and Cl is fixed at 0.07 L/h. Since in three cases the half time $t_{1/2}$ of the concentration $D_1(t)$ in the plasma compartment is much shorter than that of $D_2(t)$ in the brain compartment, so that $D_1(t) \approx 10^{-3}$ for most over the interval, $D_2(t)/D_1(t) \approx D_2(t)\times 10^3$, the shape of the corresponding graphs on the left and on the right is very similar.

We see that in all cases $\beta+\gamma < \alpha$, so that the elimination rate is given by $\beta+\gamma$. As PS decreases, β decreases and hence $\beta+\gamma$ decreases. Therefore, at each step, the half-time increases by about a factor of 10. We also observe that the limit of $D_2(t)$ drops as PS decreases, in agreement with (8.20).

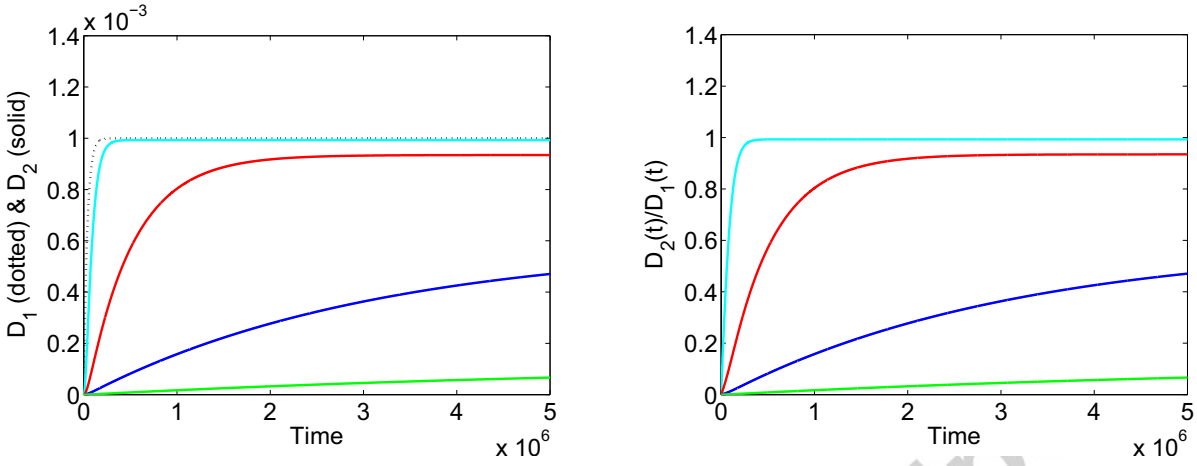

Figure 13: Graphs of $D_1(t)$ (dotted) and $D_2(t)$ (solid) on the left and $D_2(t)/D_1(t)$ on the right (over $\pm$ 140 h) for $PS = 10$ (aqua), 1 (red), 0.1 (blue) and 0.01 (green) L/h. In addition we assume that $k_{\text{infus}} = 0.00002 \times k_{\text{out}}$ (so that $D_{1,\text{ss}} = 10^{-3}$), $K_P = 1$ and $K_L = 10$. For these values we have $\alpha \approx 2.7 \times 10^{-5}$, $\beta \approx 2 \times 10^{-5}$ when $PS = 10$ L/h, and $\gamma \approx 1.4 \times 10^{-7}$. Time in seconds.

9 Discussion

In order to extend our previous one-compartment model to allow for the exploration of the impact of (i) receptors being in a compartment that is separate from the plasma compartment, and (ii) of drug binding to lipids (cf. Figure 1), we have made certain simplifying assumptions. Principal amongst these is that the behaviour of a drug in vivo can be described by simple mass action binding kinetics and that the tissue behaves as a well-stirred homogenous solution. Although there is ample precedent, this assumption being the basis of many PBPK models (Rodgers, et al. (2005)), it remains a caveat. Theoretically, more than one binding site per HSA molecule may be observed, rendering certain assumptions in the model inappropriate. However, in principle this can be determined via surface plasmon resonance (or other technology) and the model extended to allow these additional parameters to be accounted for. Accepting these assumptions as a basis for our extended model, we have found that the dissociation constant K_L for lipid binding strongly influences the dynamics of the system.

Another is the assumption of s single plasma compartment between the administration of the drug and the brain compartment. Other organs may play a role. One way one may account for this is by expanding the plasma volume V_1 to the steady state volume of distribution V_{ss}. However, this raises the question as to the size of V_{ss}. To avoid this question we envisage a sequel to this study in which additional compartments will be included. Thus, in this paper we have worked with the plasma volume V_1.

With the qualifications imposed by the assumptions discussed above, we can now draw a number of conclusions from this model. We first make a few qualitative observations.

1. Impact of K_L: We note that as the drug-affinity for the lipids increases, i.e., as K_L decreases, the long term elimination rate of the drug decreases and, in the case of

a constant rate drug infusion, the time to equilibrium increases. This is to be expected, since, as K_L decreases, the drug binds more tightly to the lipids and hence is more slowly released, causing a delay in elimination and a larger half-time.

2. Impact of two compartments: We note an important qualitative difference in the receptor occupancy curves between the one-compartment model involving proteins and receptors only and the more complex two-compartment model involving lipids as well. In the one-compartment model the AUC of the receptor occupancy curve ($AUCRO$) becomes quite small as $K_P \to \infty$, whilst in the two-compartment model the AUC of the receptor occupancy curve stays well away from zero. This can be explained by the presence of the lipids in the brain compartment, which keep the drug in that compartment, where it then remains available for the receptor.

3. The *Sweet Spot*: We observe that the *Sweet Spot* - the interior maximum of the graph of $AUCRO$ over 24 hr *versus* K_P - is present in both the one- and the two-compartment model, albeit in the two-compartment model only when K_L is large enough. In other words, if K_L is large enough, there exists a *positive* value of K_P for which the $AUCRO$ over a period of 24 h is maximal.

Not only do we make qualitative observations in the simulations of the extended system, but we also derive *explicit* approximations for the concentrations of the different compounds. They make it possible to gain insight in the role played by the different rate constants, the permeability and the initial concentrations, and actually make quantitative predictions. In particular we show that the large time behaviour is to a large extent determined by the following two *critical elimination rates*:

$$\alpha = \frac{K_P}{P_{1,0}} k_{\text{out}} \qquad \text{and} \qquad \beta = \left(1 + \frac{P_{2,0}}{K_P} + \frac{L_{2,0}}{K_L}\right)^{-1} \frac{PS}{V_2} \tag{9.1}$$

where α only contains parameters related to the plasma compartment and β only contains parameters related to the brain compartment.

4. Elimination: The terminal slope (λ_z) of the system is given by

$$\lambda_z = \alpha \ \text{ if } \ \alpha < \beta \qquad \text{and} \qquad \lambda_z = \beta \ \text{ if } \ \alpha > \beta \tag{9.2}$$

When drug is administered through a constant rate infusion, we find that the drug concentrations in both compartments eventually equalise. Specifically,

5. Equilibration: For constant rate infusion, the free drug concentration will equilibrate between brain and plasma for all non-zero permeability values, i.e.,

$$\frac{D_2(t)}{D_1(t)} \to 1 \qquad \text{as} \qquad t \to \infty. \tag{9.3}$$

The permeability of the membrane, and the protein and lipid binding influence the time to equilibrium – through α or β, depending on which is the smallest – but not the limit of D_2/D_1. Since many drugs are given over weeks, if not months and years, over time the drug in the plasma and the brain achieves a pseudo steady state.

Thus, according to the model sketched in Figure 1, free drug could achieve equilibrium; indeed as the blood-brain barrier in man is very large – of the order of 200,000 cm^2 (cf. Goodwin et al. (2005)) – then from equation (9.2) it can be calculated that even drugs with low values of permeability (e.g. 10^{-6} cm/s, which translates into a PS value of 0.7 L/h) and typical lipid and protein binding should achieve equilibrium within a time frame of days. Note that the permeability of drugs can be measured and is typically reported as between 0.3 and 3×10^{-4} cm/s (cf. Fagerholm (2007) and Lundquist et al. (2002)). Taken together, this assessment of inter-compartmental equilibration processes would appear to challenge the notion (cf. Pardridge (2007)) that achieving brain penetration and receptor occupancy will be challenging. On the contrary, this appears to suggest that restricting drug from the brain is more likely to be an issue, if required.

However, the model of Figure 1 does not take into account processes that remove drug from the brain. Two examples of this are known; bulk flow from the CSF to the plasma and active transporter-mediated processes.

We estimate that the bulk flow from the CSF is of the order of 0.07 L/h. If, for example, restriction of drug from brain is required with free brain/plasma ratio of 0.1, then PS would need to be $1/10^{th}$ of CL_{CSF} (0.007 L/h) and from the paragraph above we see that the permeability would have to be 1×10^{-8} cm/s. This conclusion is consistent with published in vivo work showing poorly penetrating compounds such as *sucrose* and *mannitol* exhibiting permeabilities in the range $1 \times 10^{-7} - 1 \times 10^{-8}$ cm/s (Takasato et al. (1984)).

On- *versus* off-rates: Drug receptor interactions are often described in terms of equilibrium affinity measures such as K_R or IC_{50}. However, it has been argued that the rate constants for a given reaction equilibrium are important determinants of pharmacodynamic behaviour, in particular the off rate for binding (cf. Tummino and Copeland (2008)). Hence, a question that arises in the process of drug discovery is whether the off-rate is a selectable parameter and moreover would this necessarily be correlated with affinity. For example, in the simplest case of a one step binding as in equation (2.2), the ratio of the off- and on-rates equals the equilibrium binding constant. Hence, one strategy to decrease the off-rate would be to increase the affinity of a drug, on the assumption that the on-rate is a relatively constant parameter (cf. Tummino and Copeland (2008)). Alternatively, it could be argued that for a given affinity, an infinite spectrum of on- and off-rate parameters could yield an equal affinity value. This implies that determining on- and off-rates for a range of candidate drugs could be useful, if it turns out that drugs with equal K_R-value but specific combinations of on- and off-rates have improved pharmacodynamic outcome. Clearly this is potentially a complex question to address for an open system such as the in vivo situation, but in the models described in this paper it is possible to explore this question in the context of a simple model of drug disposition. Hence, we simulated the impact of a range of off- and on-rates, yielding the same K_R parameter (0.001 μM) and for typical drug characteristics. The results in Figure 14 show negligible impact of varying rates over three orders of magnitude. This lack of impact can be understood when we realise that the analytical approximations for the drug concentrations only depend on the value of the quotient of the off- and on-rate, i.e., the affinity K_R.

We infer from this that although sustained residence time on the receptor may be

desirable, at least under the conditions adopted in this paper, selecting a drug with slower off-rate at the expense of on-rate has no benefit. How generic this conclusion is remains to be determined, but the models described here may be used to explore this for a wider range of drug properties.

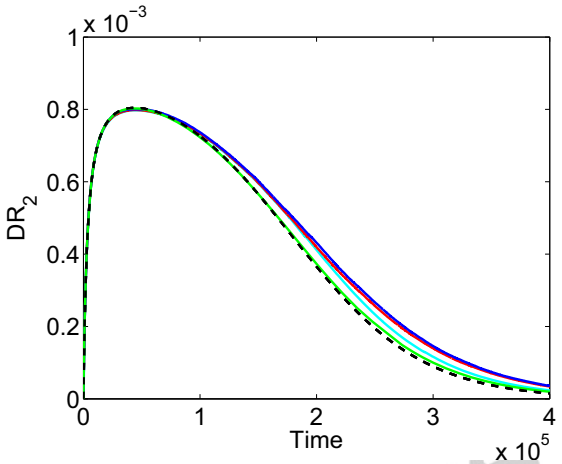

Figure 14: Graphs of DR_2 versus time over $\pm$ 110 hours – numerical (solid) and analytical (dashed) – for $k_{\mathrm{Rf}} = 10^n$, $n = 4$, 5, 6, 7 and k_{Rb} is chosen so that in each simulation $K_R = 10^{-3}$. In addition we have $K_P = 1$, $K_L = 10$, $k_{\mathrm{out}} = 0.02$ and $D_{1,0} = 10$ (see also Tables 1 and 2).

In this manuscript we have developed and explored some of the behaviours of a model of the pharmacokinetics, inter-compartmental distribution and receptor binding of a drug in the presence of proteins and lipids. The model facilitated the exploration of this complex problem and revealed that (*i*) contrary to some hypotheses, restricting a drug from the brain may be challenging, unless an active brain clearance process is involved, (*ii*) drug binding to lipids competes with binding to proteins and, in particular, in the brain compartment it is the limiting factor for the elimination rate, and the time to equilibrium in the event of a constant rate drug infusion and (*iii*) optimising PKPD properties through slow-offset from the receptor alone may not always be a feasible strategy for CNS drugs.

References

Berezhkovskiy, L.M., 2004. Volume of distribution at steady state for linear pharmcokinetic system with peripheral elimination. J. Pharm. Sciences 93 (6), 1628-1640.

Berezhkovskiy, L.M., 2010. On the influence of protein binding on pharmacological activity of drugs. J. Pharm. Sciences 99 (4), 2153-2165.

Blanchard, P., Devaney, R.J., Hall, D.R., 1998. Differential equations. Brooks/Cole PublishingCompany, Pacific Grove, California.

Fagerholm, U., 2007. The highly permeable blood-brain barrier: an evaluation of current opinions about brain uptake capacity. Drug Discovery today 12 (23/24), 1076-1082.

Felgenhauer, K., 1974. Protein size and cerebrospinal fluid composition. Klin. Wochenschr. 52 (24), 1158-1164.

Frostell-Karlsson, A., Remaeus, A., Roos, H., Andersson, K., Borg, P., Hamalainen, M., Karlsson, R., 2000. Biosensor analysis of the interaction between immobilised human serum albumin and drug compounds for prediction of human serum albumin binding levels. J. Medicinal Chem. 43 (10), 1986-92.

Gervasini, G., Carrillo, J.A., Benitez, J., 2004. Potential role of the cerebral cytochrome P450 in clinical pharmacokinetics. Clin. Pharmacokinet. 43, 693-706.

Ghose, G.K., Viswanadhan, V.N., Wendoloski, J.J., 1999. A knowledge-based approach in designing combinatorial or medicinal chemistry libraries for drug discovery. J. Combin. Chem. 1, 55-68.

Goodwin, J.T., Clark, D.E., 2005. In silico predictions of blood-brain barrier penetration: considerations to "keep in mind". J. Pharmacol. Exp. Ther. 315 (2), 477-483.

Grant, R., Condon, B., Patterson, J., Wyper, D.J., Hadley, M.D., Teasdale, G.M., 1989. Changes in cranial CSF volume during hypercapnia and hypocapnia. J Neurol. Neurosurg. Psychiatry 52, 218-222.

Guyton, A.C., Hall, J.E., 1996. Textbook of medical physiology. 9th ed.; W.B. Saunders, Philadelphia, pp. 161-164.

Hammarlund-Udenaes, M., Fridén, M., Styvänen, S., Gupta, A., 2008. On the rate and extent of drug delivery to the brain. Pharm. Research 25 (8), 1737-1750.

Jusko, W.J., 1995. Pharmacokinetics and receptor-mediated pharmacodynamics of corticosteroids. Toxicology 102(1-2), 189-96.

Lundquist, S., Renftel, M., Brillault, J., Fenart, L., Cecchelli, R., Dehouck, M.P., 2002. Prediction of drug transport through the blood-brain barrier in vivo: a comparison between two in vitro cell models. Pharm. Research 19 (7), 976-981.

Motulsky, H.J., Mahan, L.C., 1984. The kinetics of competitive radioligand binding predicted by the law of mass action. Mol. Pharmacol. 25 (1), 1-9.

Pardridge, W., 2007. Bloodbrain barrier delivery. Drug Discovery Today 12 (1/2), 54-61.

Peletier, L.A., Benson, N., Van der Graaf, P.H., 2009. Impact of plasma-protein binding on receptor occupancy: an analytical description. J. Theor. Biol. 256 (2), 253-62.

Poulin, P., Theil, F.P., 2000. A priori prediction of tissue:plasma partition coefficients of drugs to facilitate the use of physiologically-based pharmacokinetic models in drug discovery. J. Pharm. Sciences 89 (1), 16-35.

Rich, R.L., Day, Y.S., Morton, T.M., Myszka, D.G., 2001. High-resolution and high throughput protocols for measuring drug/Human Serum Albumin interactions using BIACORE. Anal. Biochem. 296 (2), 197-207.

Rodgers, T., Leahy, D., Rowland, M., 2005. Physiologically based pharmacokinetic modelling 1: Predicting the tissue distribution of moderate-to-strong bases. J. Pharm. Sciences 94 (6), 1259 - 1276.

Rouser, G., Yamamoto, A., 1968. Curvilinear regression course of human brain lipid composition changes with age. Lipids 3 (3), 284-287.

Schmidt, S., Gonzalez, D., Derendorf, H., 2010. Significance of protein binding in pharmacokinetics and pharmacodynamics. J. Pharm. Sciences 99 (3), 1107-1122.

Silverberga, G.D., Mayob, M., Saulc, T., Rubenstein, E., McGuireb, D., 2003. Alzheimer's disease, normal-pressure hydrocephalus, and senescent changes in CSF circulatory physiology: a hypothesis. The Lancet: Neurology 2 (8), 506-511.

Takasato, Y., Rapoport, S.I., Smith, Q.R., 1984. An in situ brain perfusion technique to study cerebrovascular transport in the rat. Am. J. Physiol. 247, H484-H493, 3.

Tummino, P.J., Copeland, R.A., 2008. Residence time of receptor-ligand complexes and its effect on biological function. Biochemistry 47 (20), 5481-92.

Whittico, M.T., Giacomini, K.M., 1988. Cimetidine Elimination from the Cerebrospinal Fluid of the Rat. Pharm. Research 5 (10), 628-633.